

Supplementary Material

Design, synthesis, and biological evaluation of novel multifunctional Rolipram-Tranilast hybrids as potential treatment for traumatic brain injury

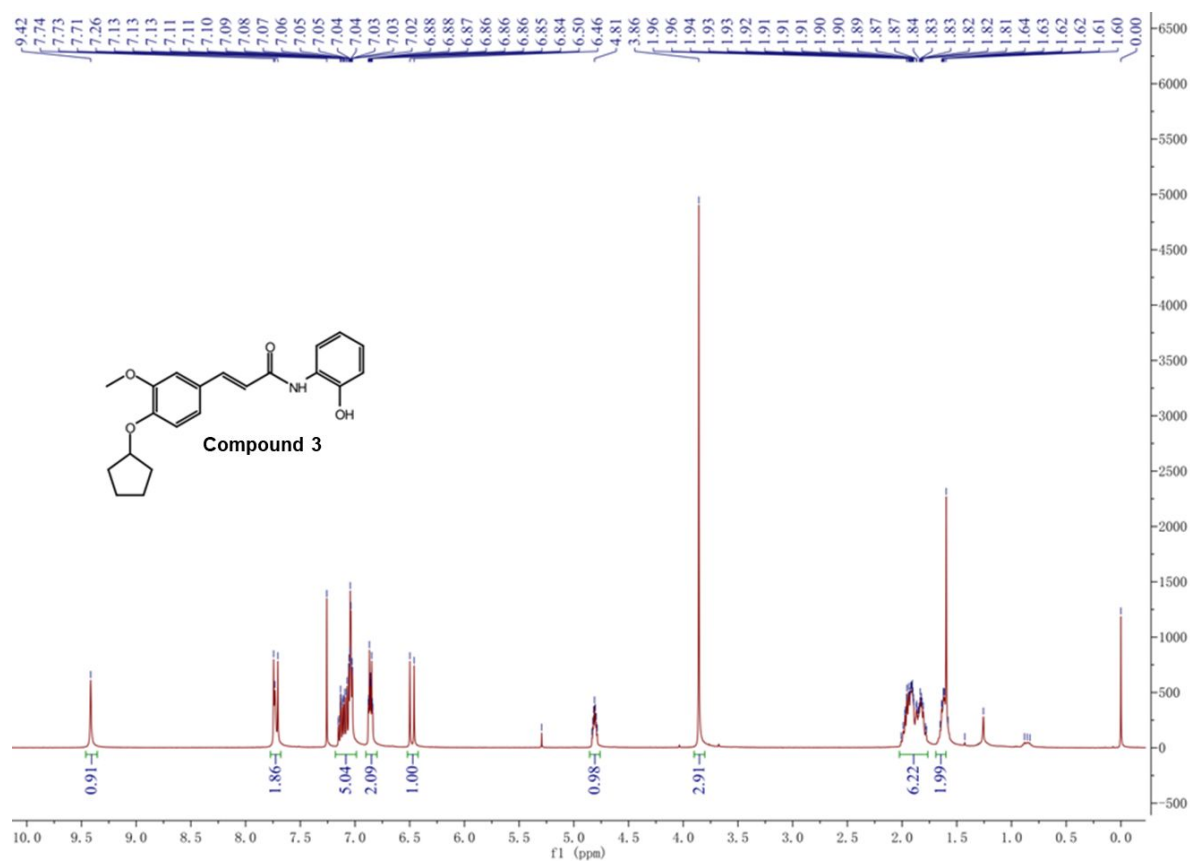
Junfeng Lu^{1§}, Chen Chen^{1§}, Xiaobing Deng^{2§}, Marvin SH Mak^{3,4}, Zeyu Zhu¹, Xixin He⁵, Jinhao Liang⁵, Swetha K. Maddili⁶, Karl W. K. Tsim⁴, Yifan Han³, Rongbiao Pi^{6,7,8*}

- 1. School of Pharmaceutical Sciences, Sun Yat-Sen University, Guangzhou 510006, China;*
- 2. Peking-Tsinghua Center for Life Sciences, Peking University, Beijing 100871, China.*
- 3. Department of Applied Biology and Chemical Technology, Institute of Modern Chinese Medicine, The Hong Kong Polytechnic University, Hung Hom, Hong Kong;*
- 4. Division of Life Science and Center for Chinese Medicine, The Hong Kong University of Science and Technology, Hong Kong, China;*
- 5. School of Pharmaceutical Sciences, Guangzhou University of Chinese Medicine, Guangzhou, China.*
- 6. School of Medicine, Sun Yat-Sen University, Guangzhou 518000, China;*
- 7. National and Local United Engineering Lab of Drugability and New Drugs Evaluation, Sun Yat-Sen University, Guangzhou 510006, China;*
- 8. International Joint Laboratory<SYSU-PolyU HK> of Novel Anti-Dementia Drugs of Guangzhou, Guangzhou 510006, China.*

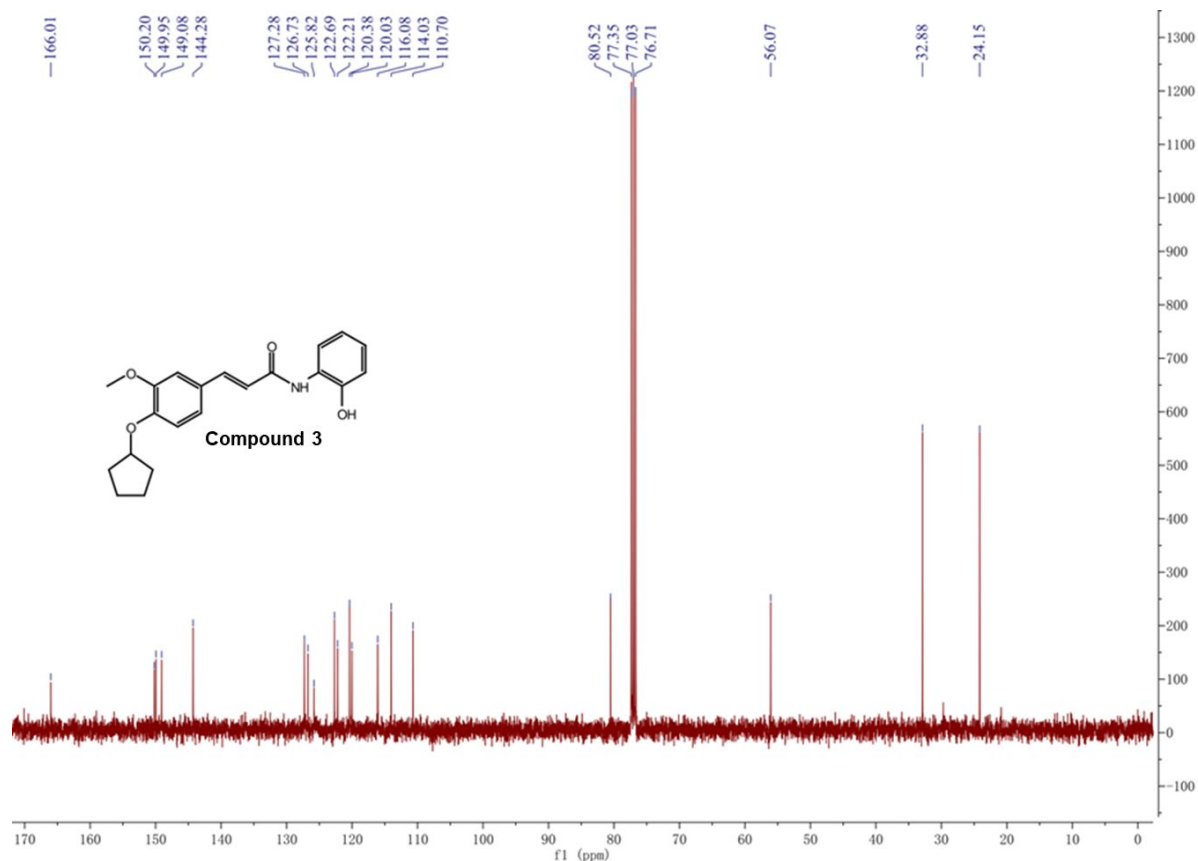
[§] The first three authors contributed equally.

Contents

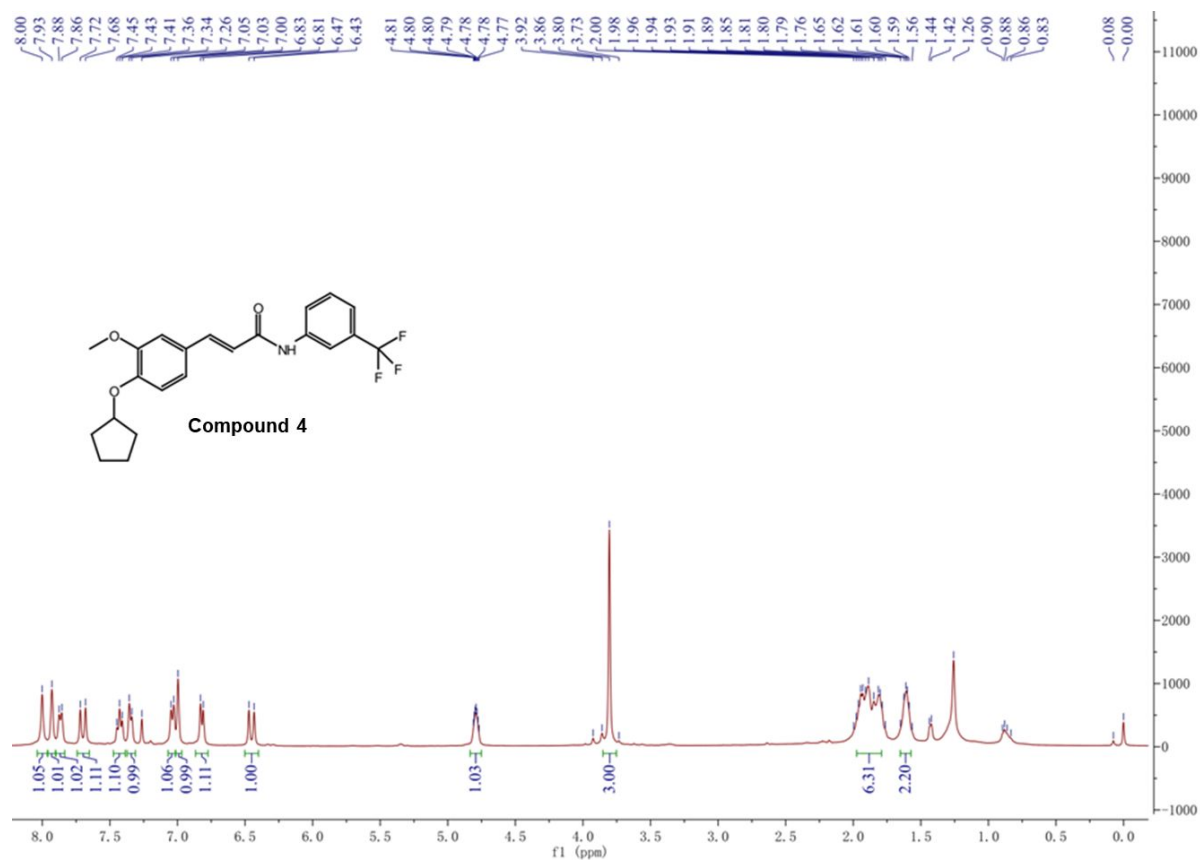
^1H NMR and ^{13}C NMR of final compounds **3-14**, **15-26**



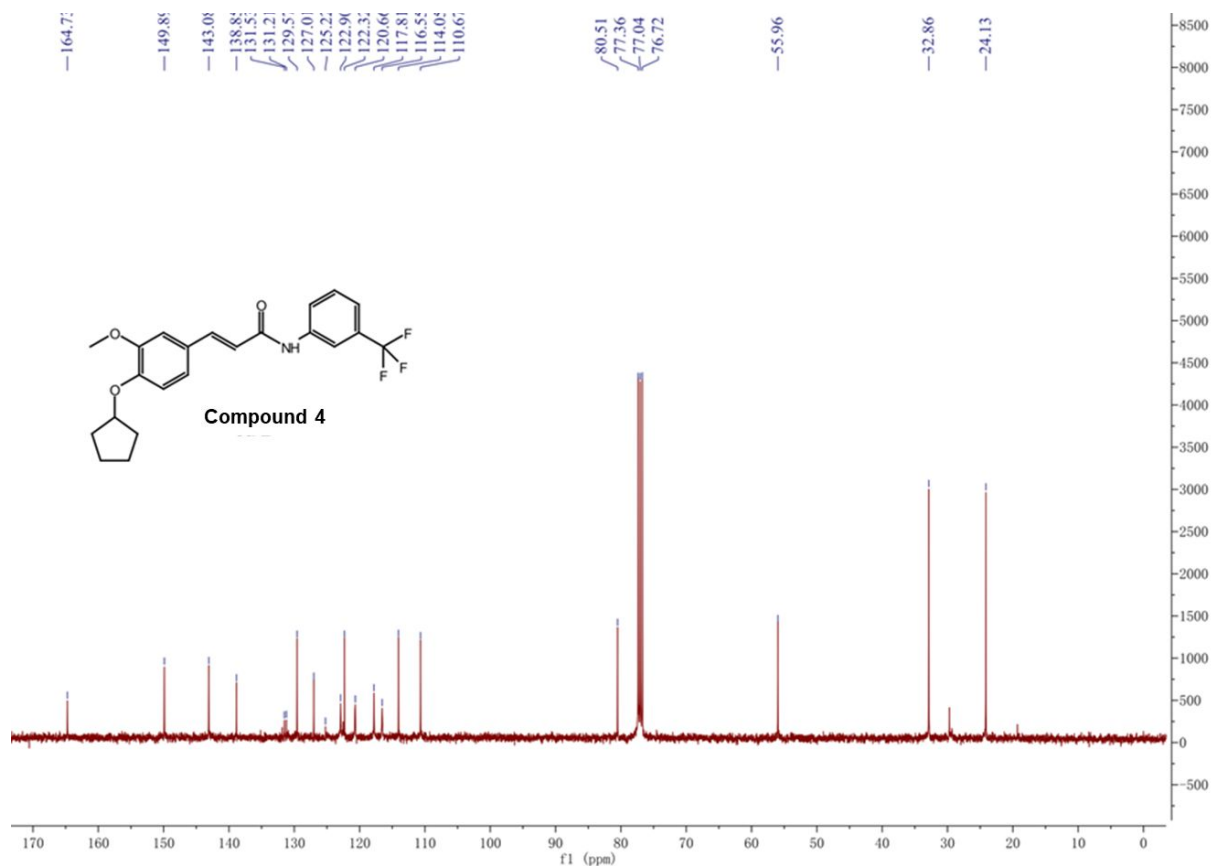
^1H NMR compound **3**



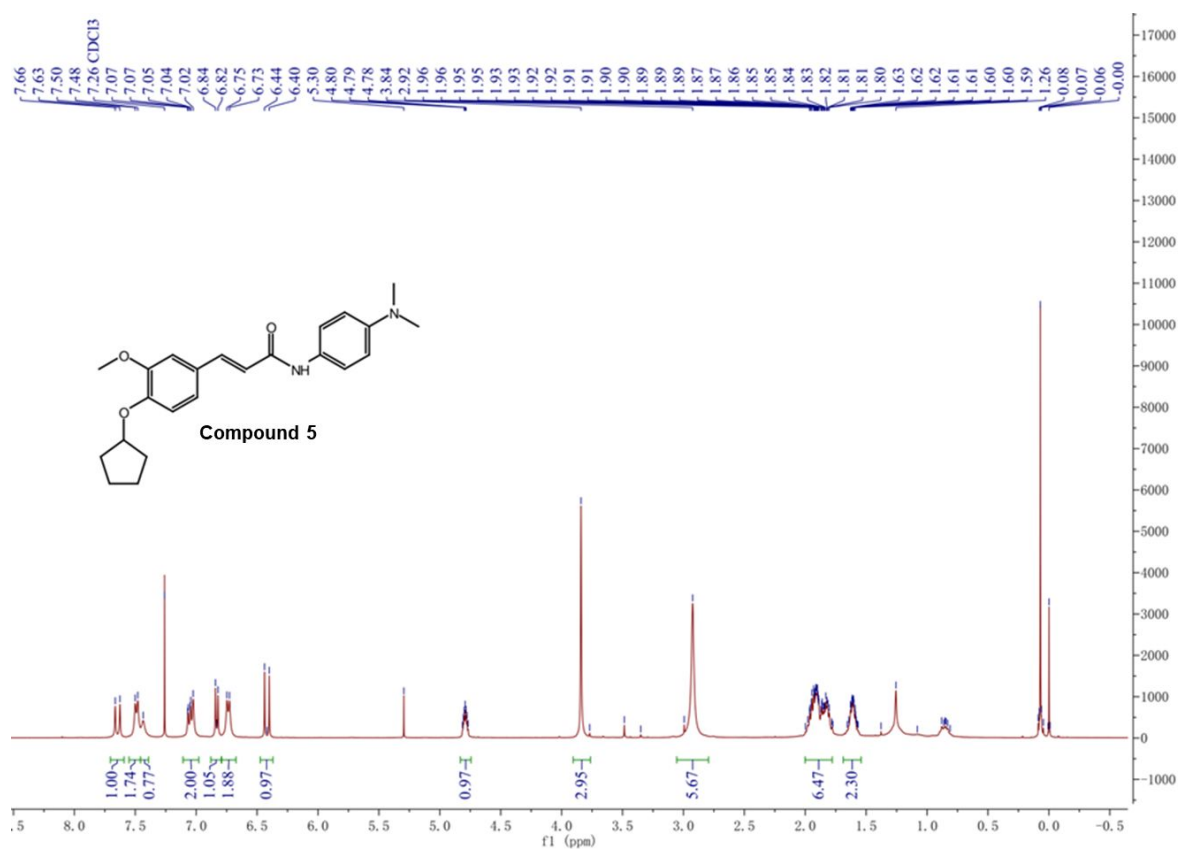
^{13}C NMR compound 3



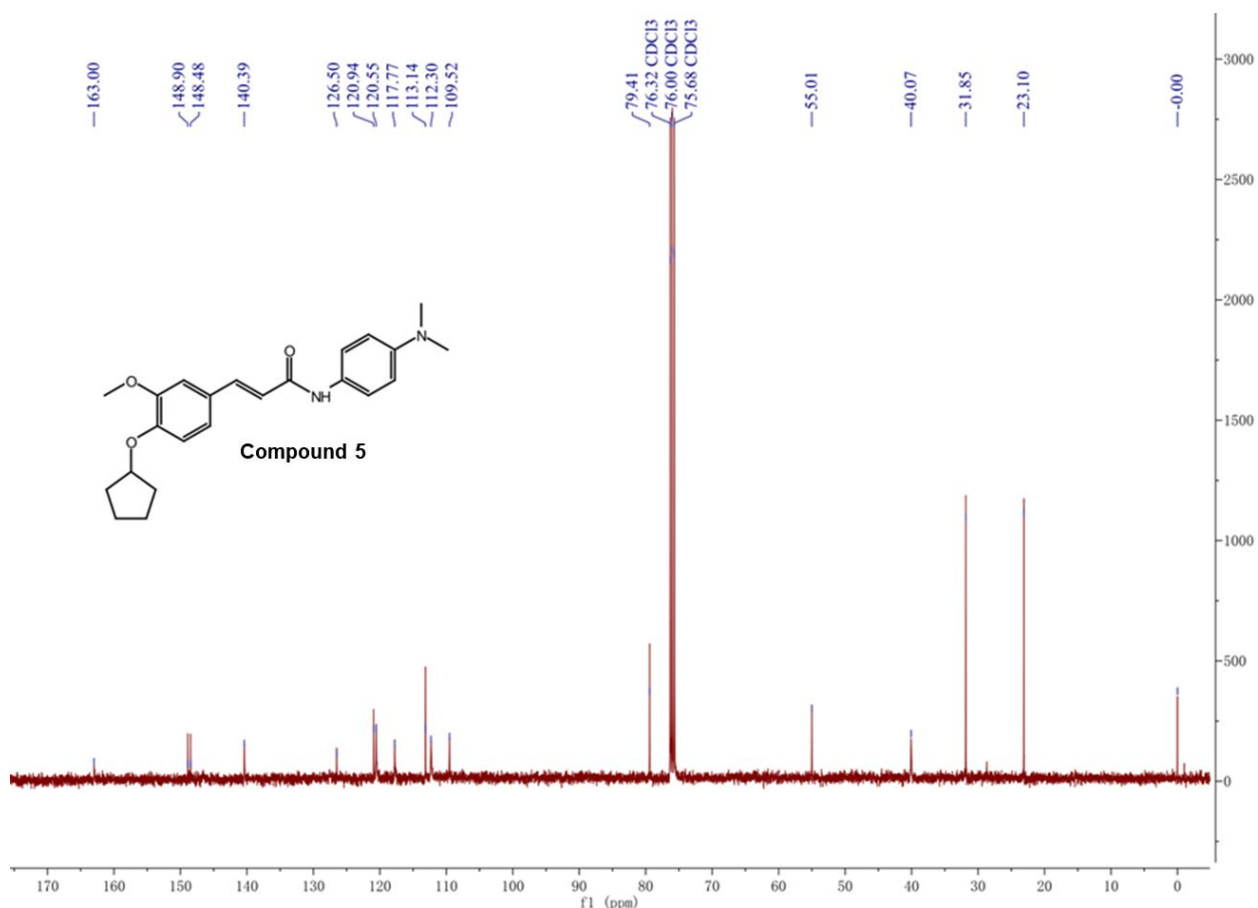
^1H NMR compound 4



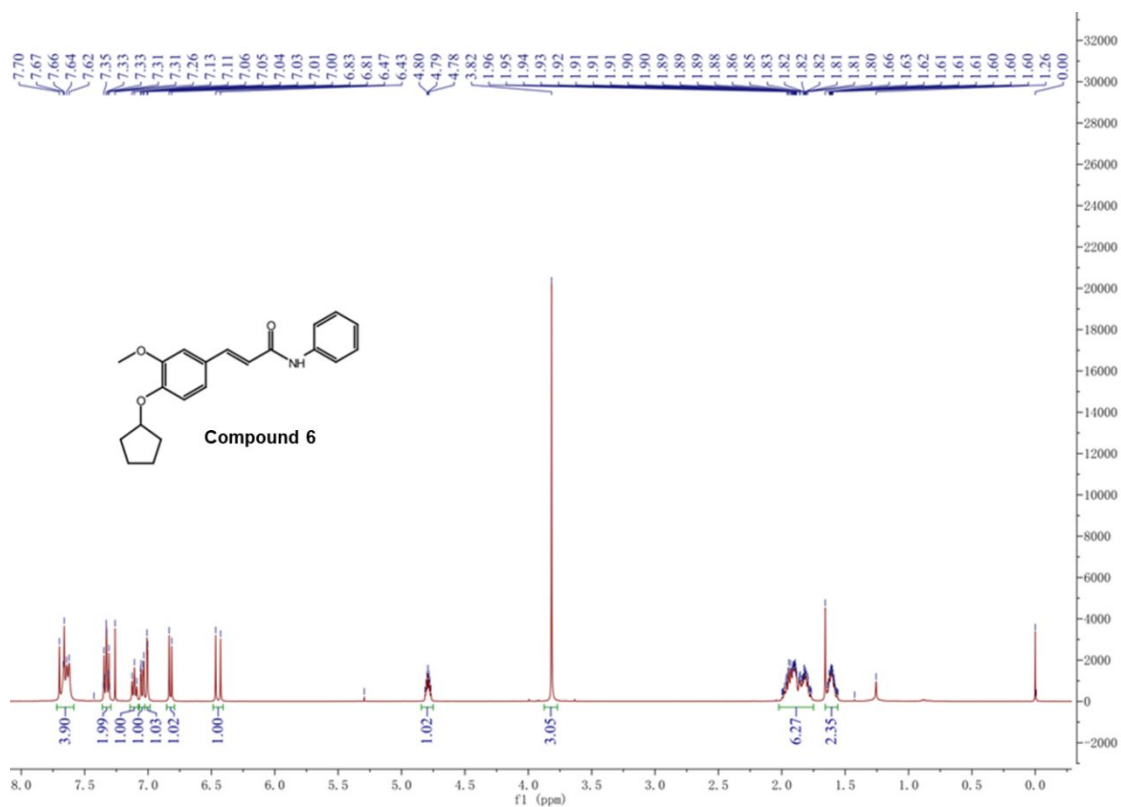
¹³C NMR compound 4



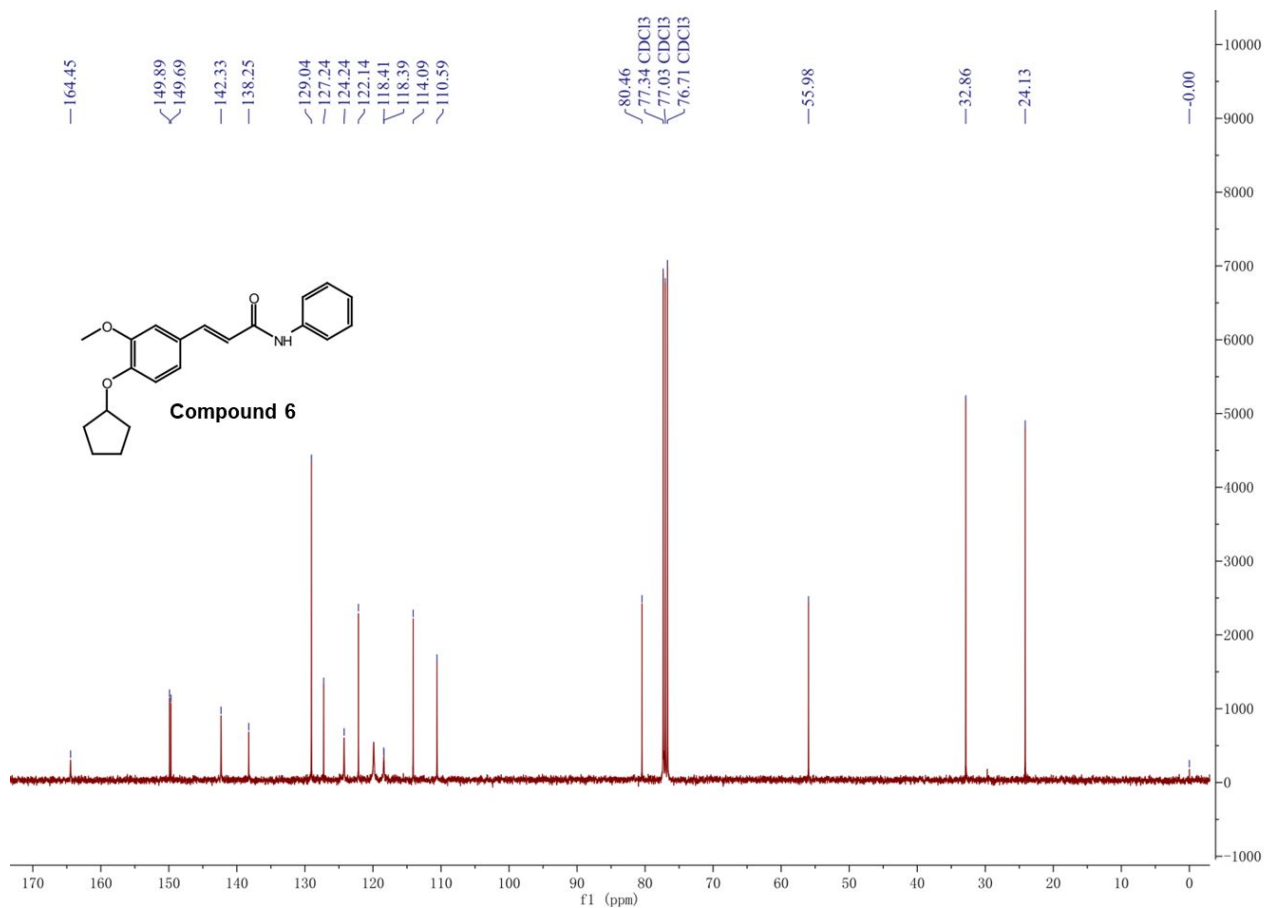
¹H NMR compound 5



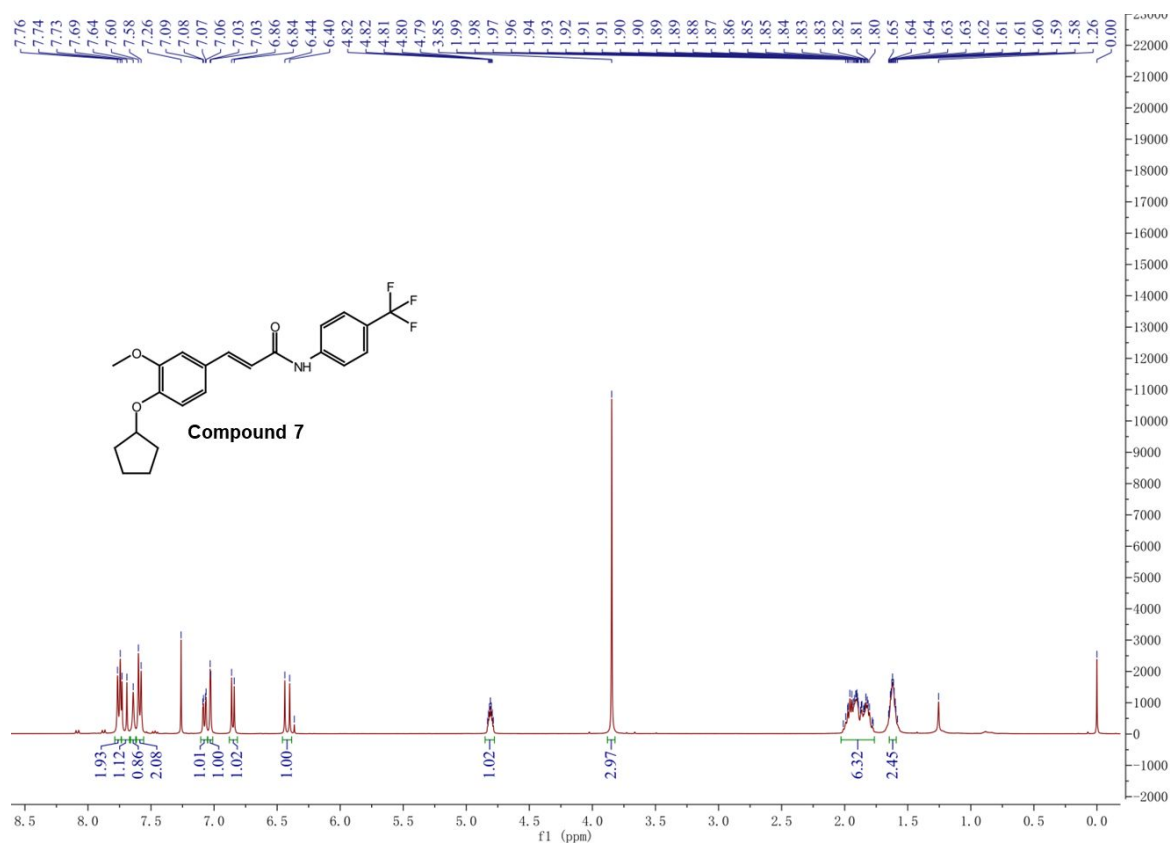
¹³C NMR compound 5



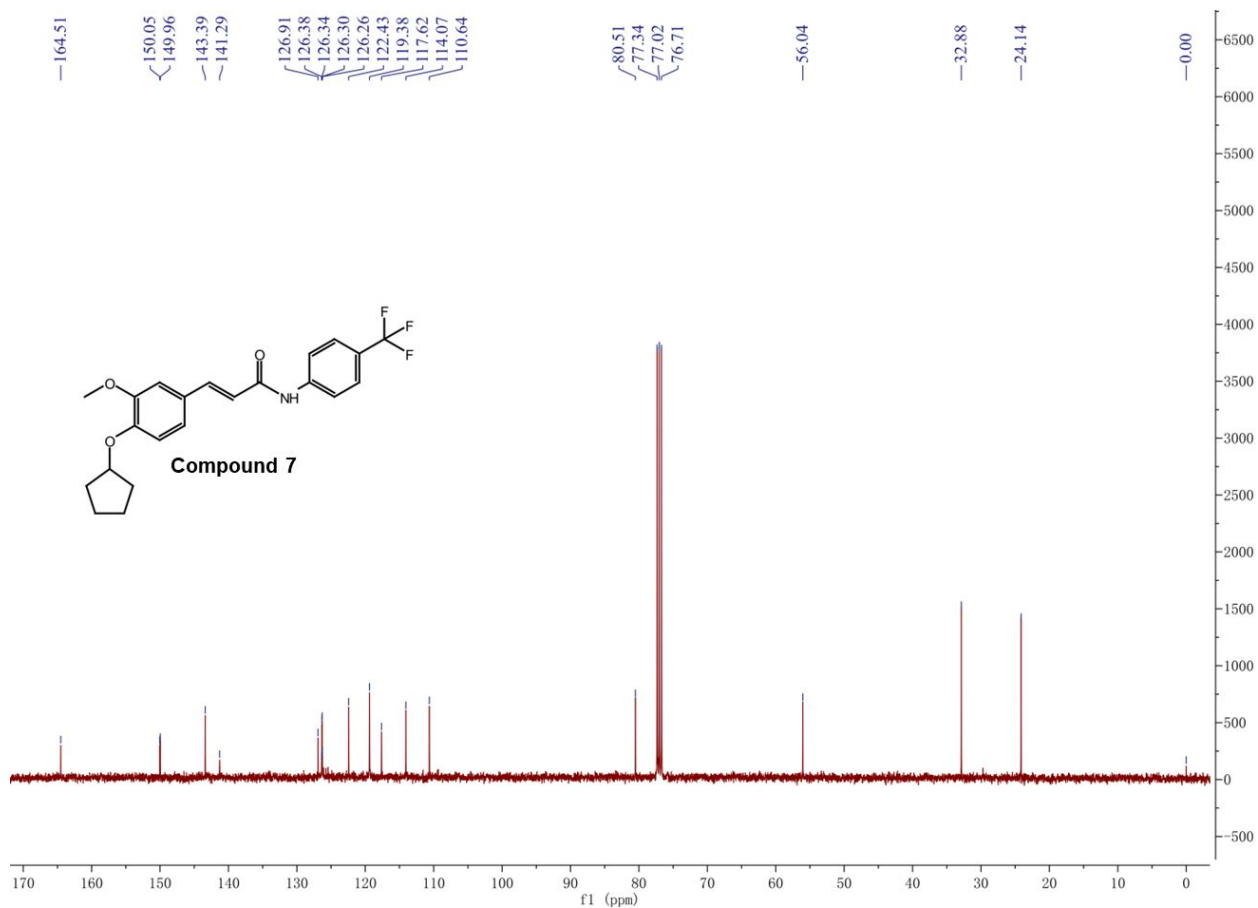
¹H NMR compound 6



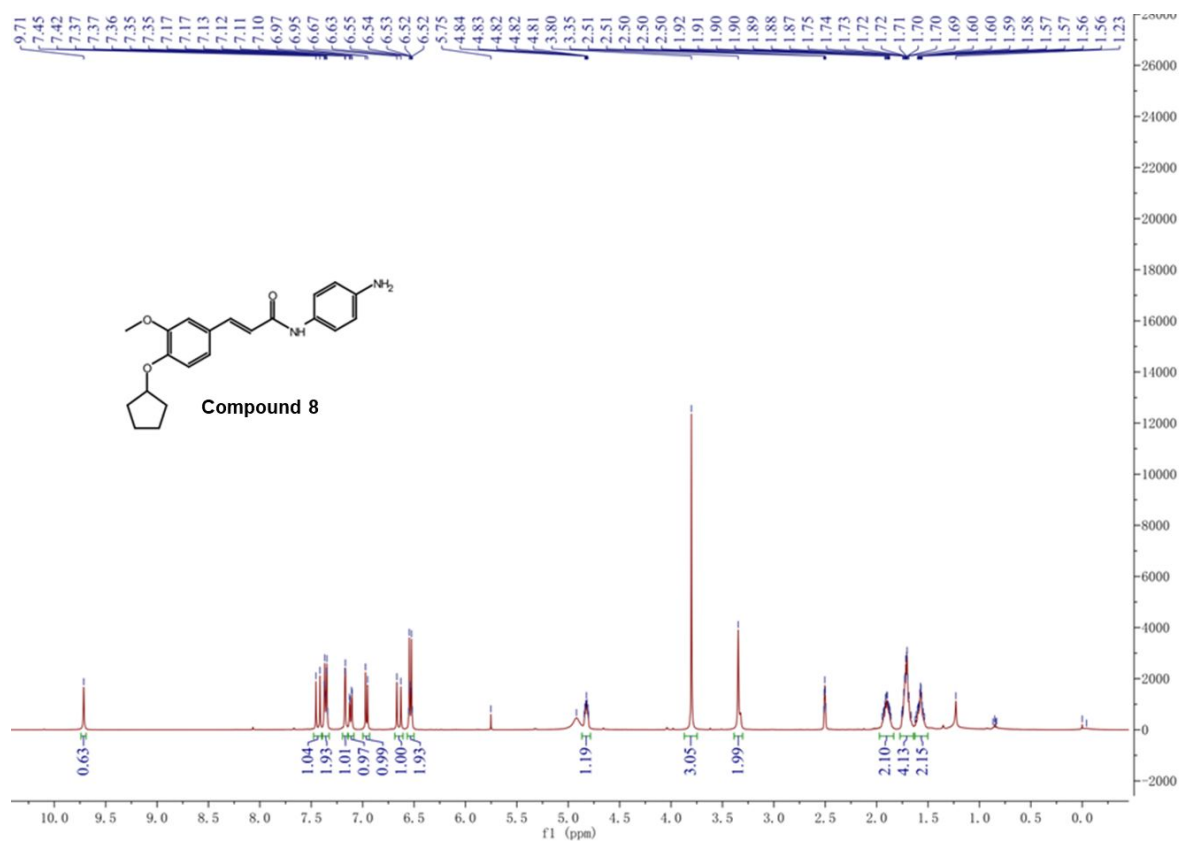
¹³C NMR compound 6



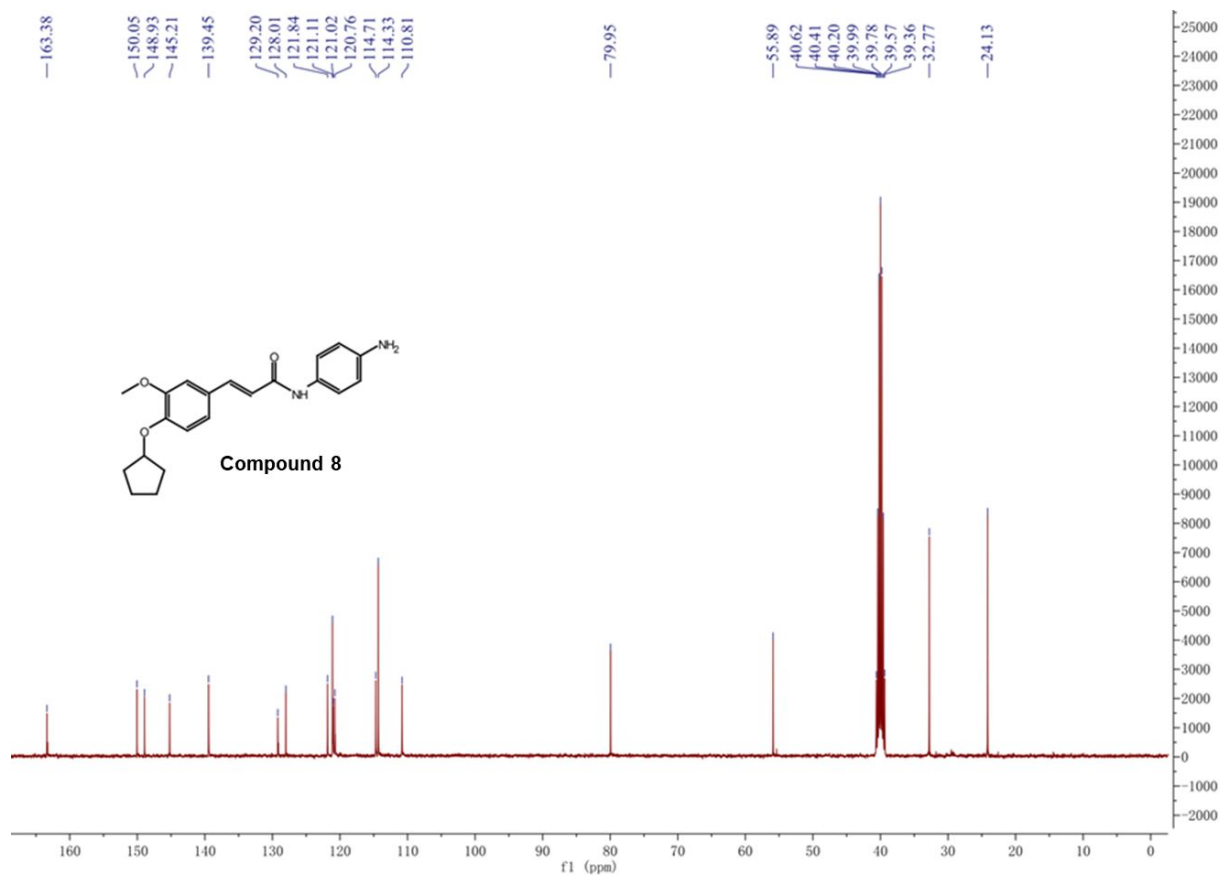
¹H NMR compound 7



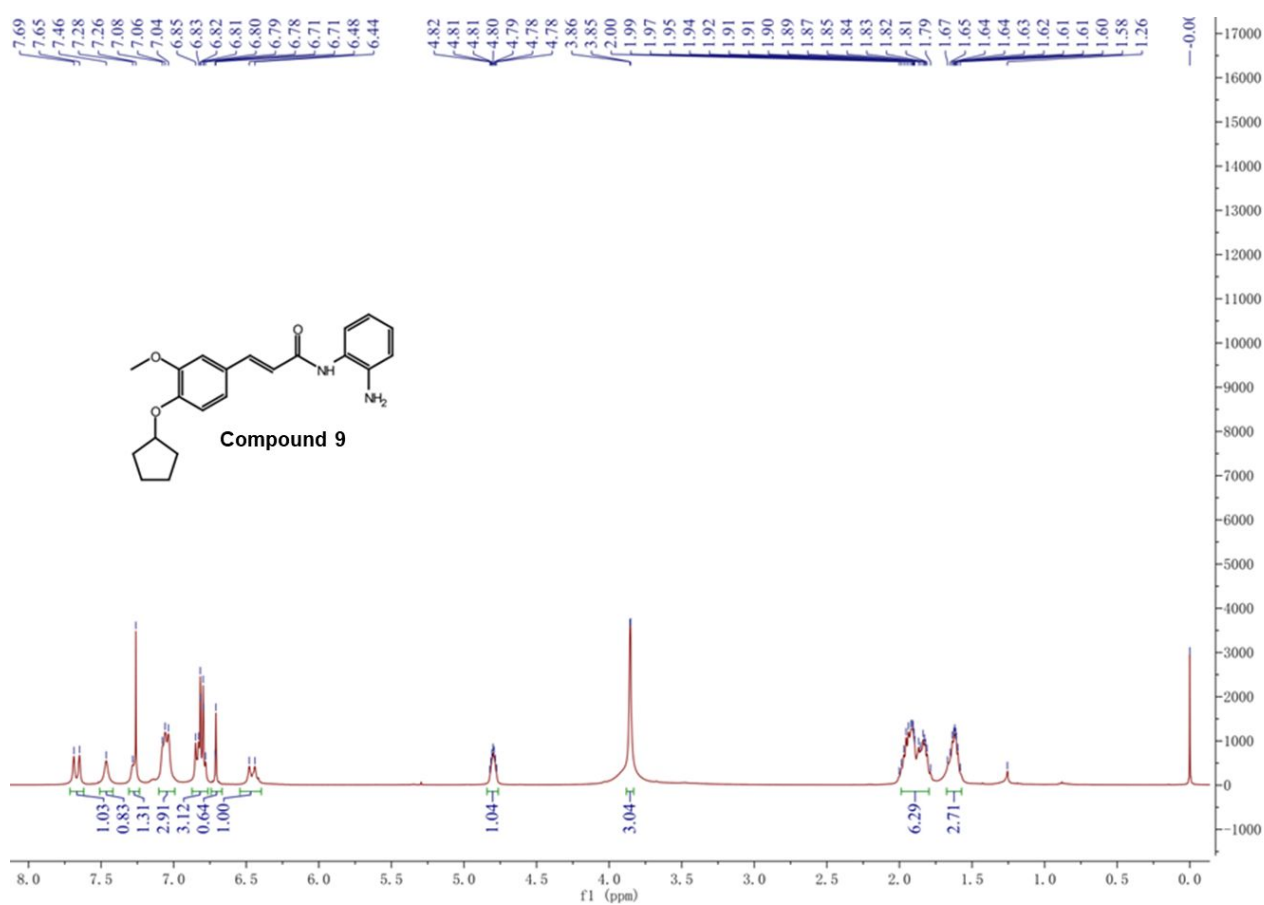
¹³C NMR compound 7



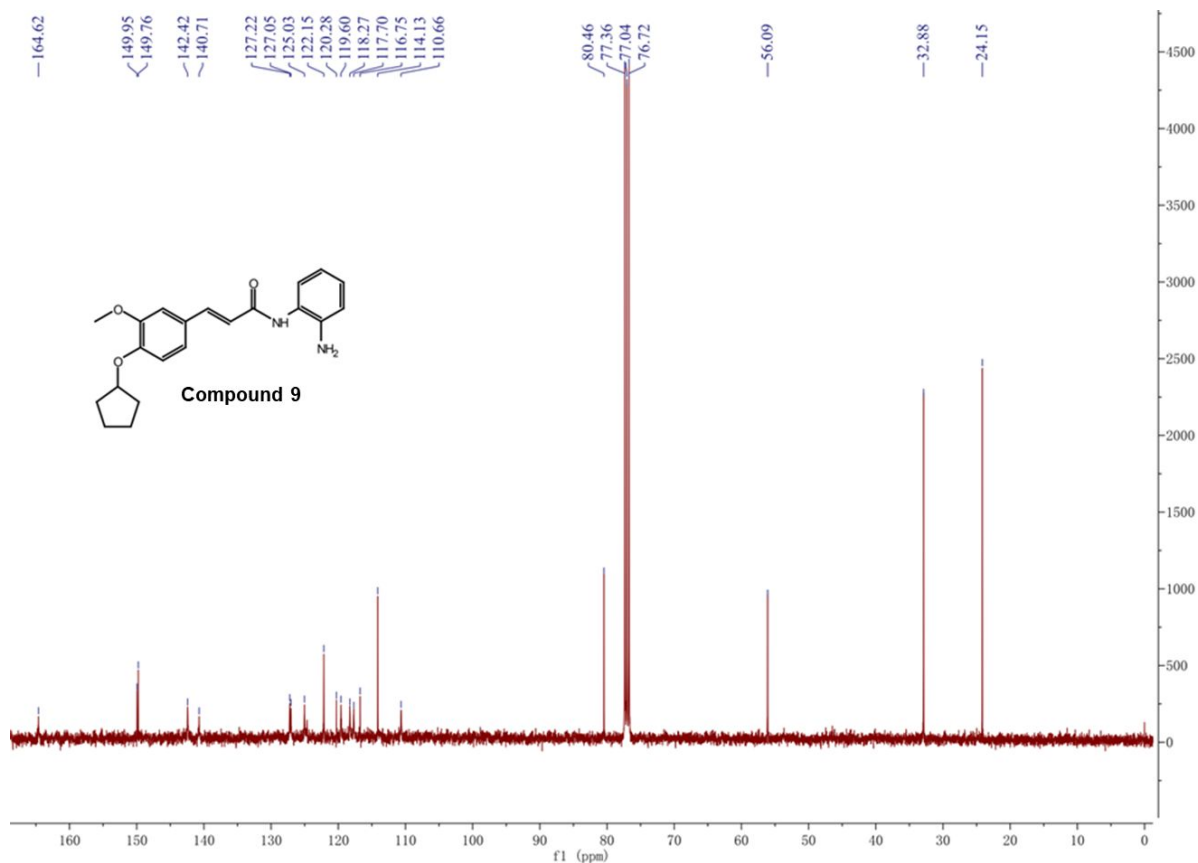
¹H NMR compound 8



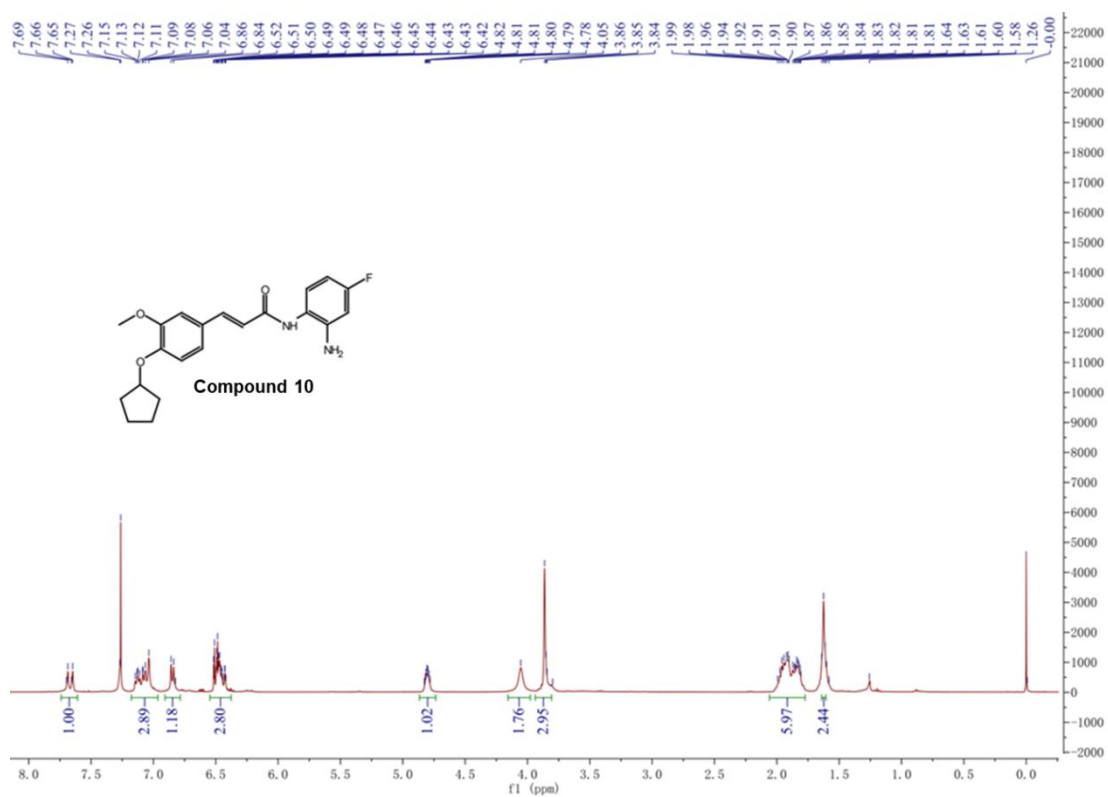
¹³C NMR compound 8



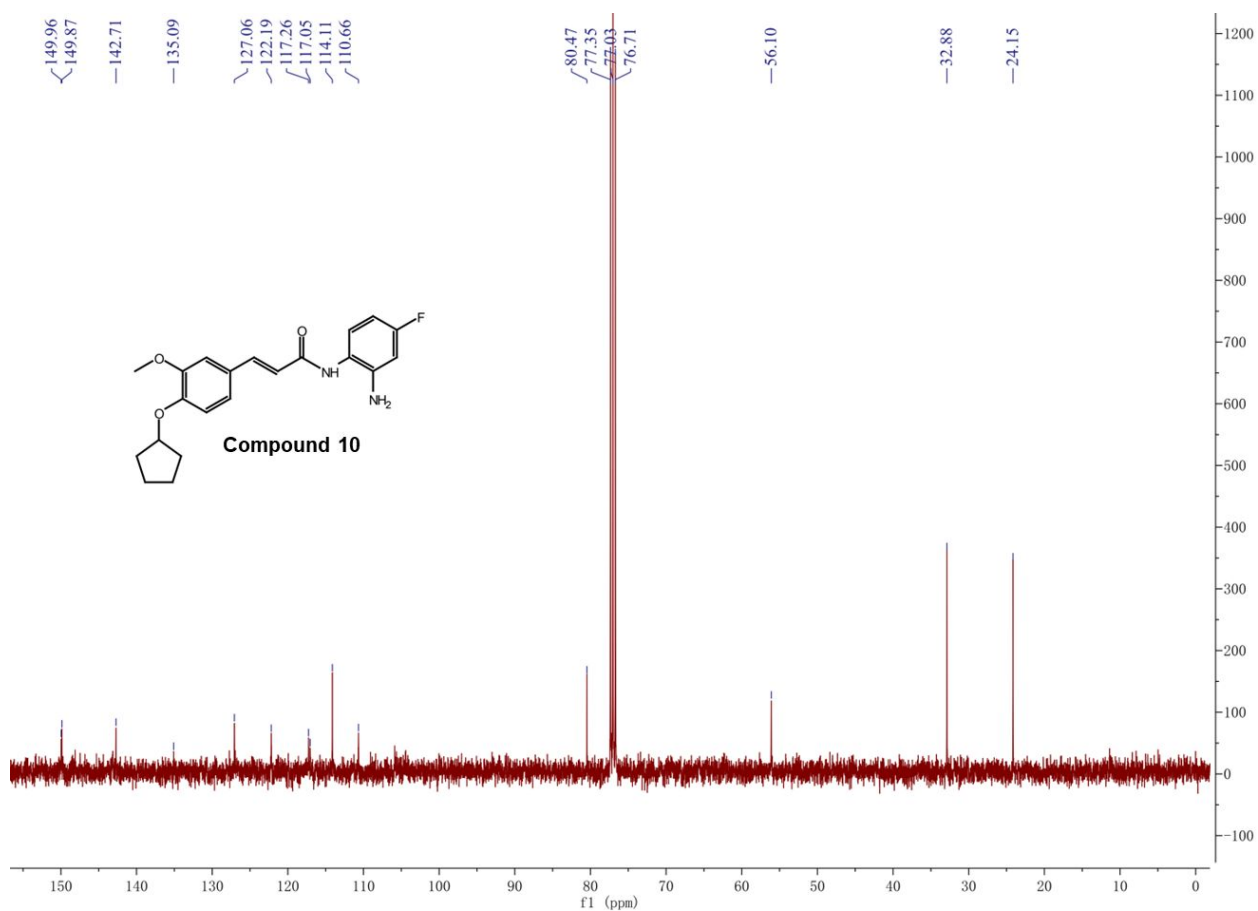
¹H NMR compound 9



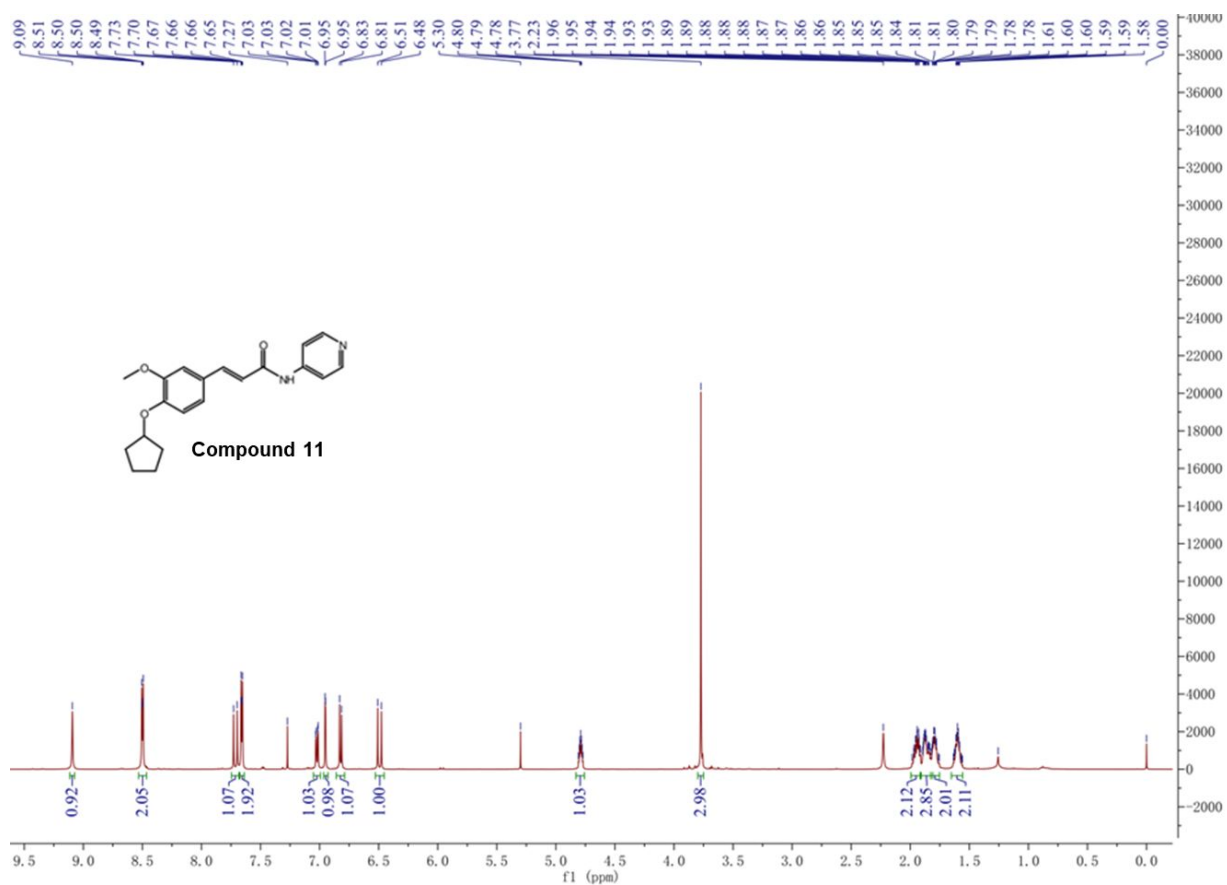
¹³C NMR compound 9



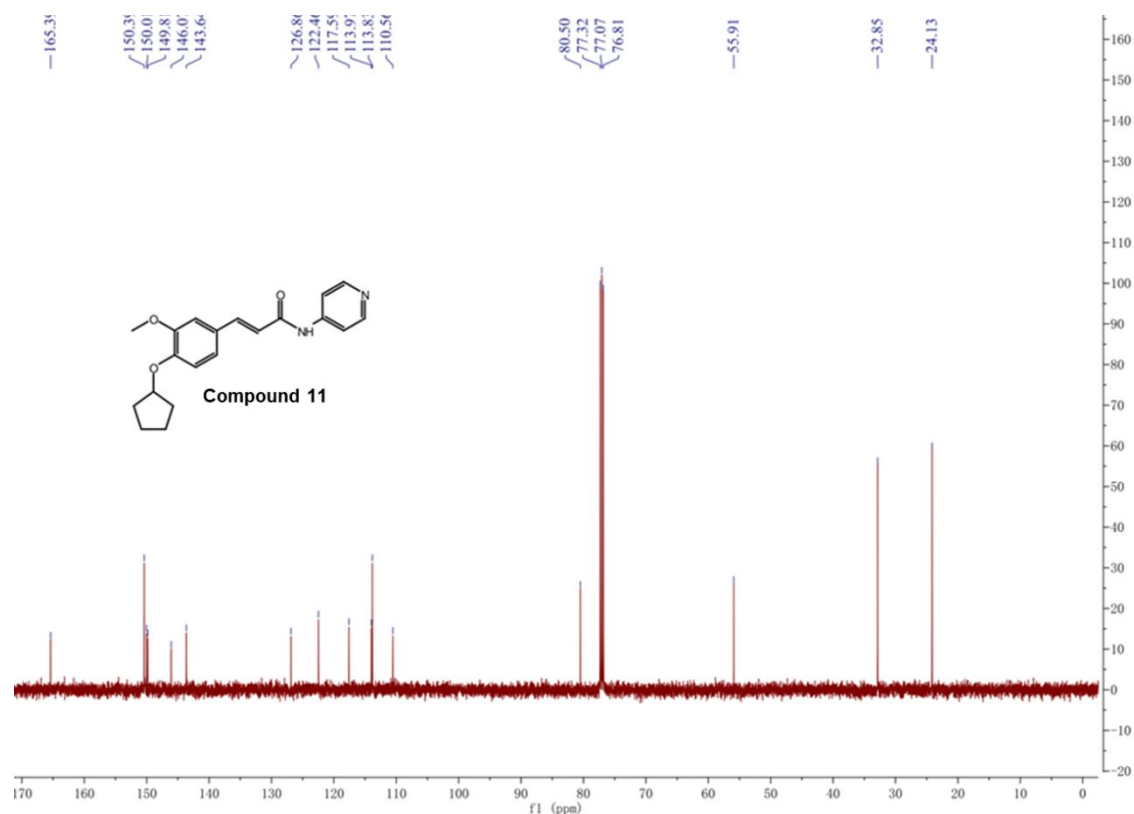
¹H NMR compound 10



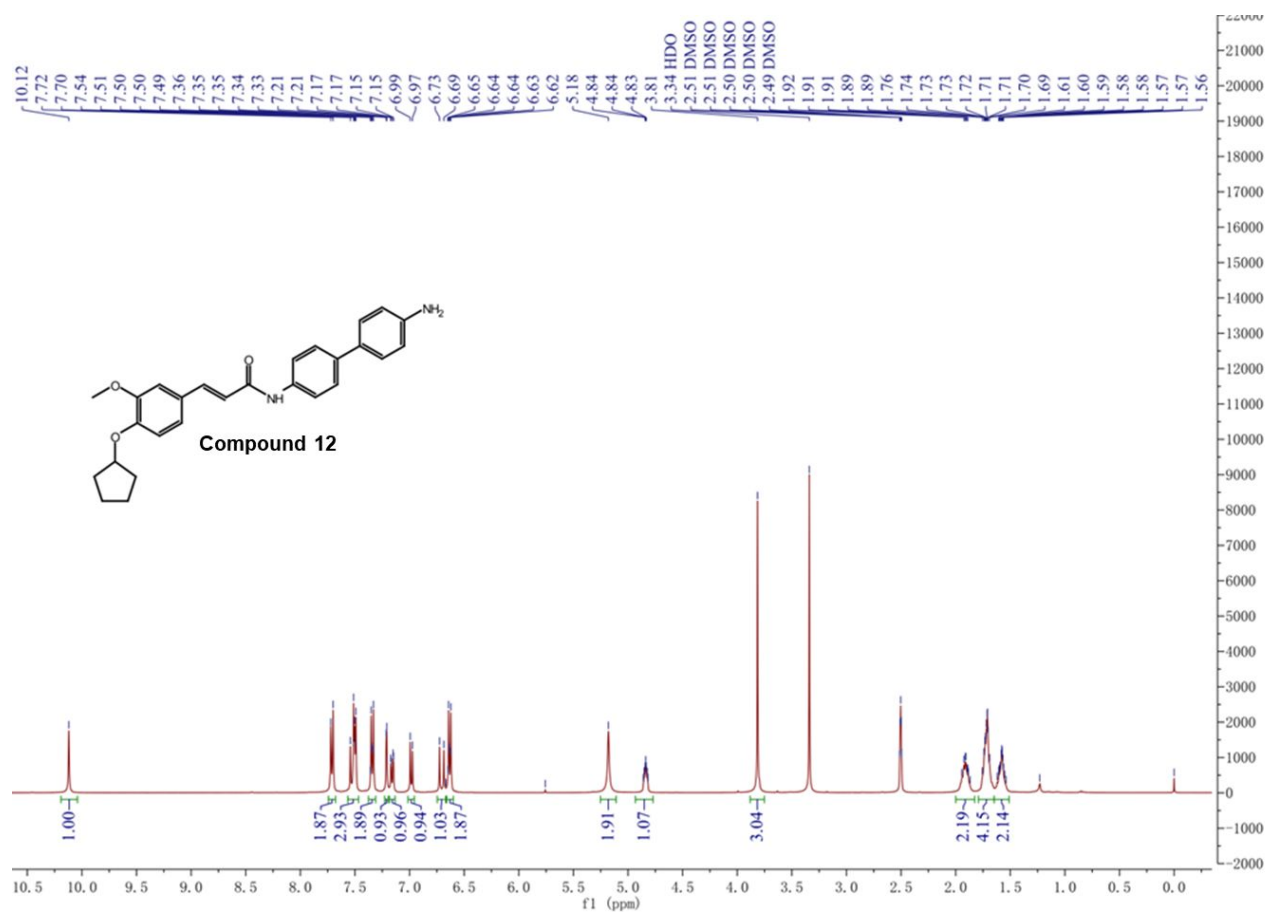
¹³C NMR compound 10



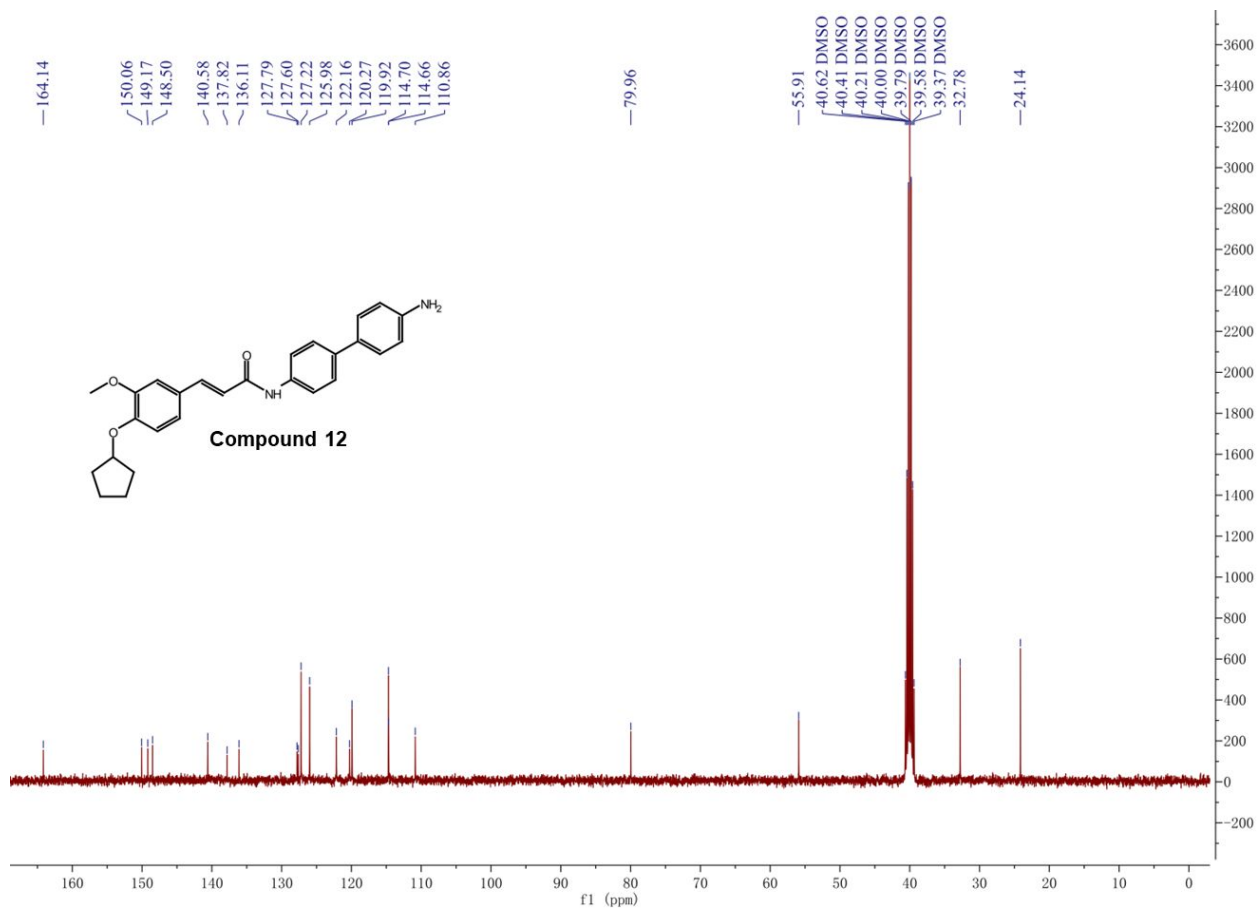
¹H NMR compound 11



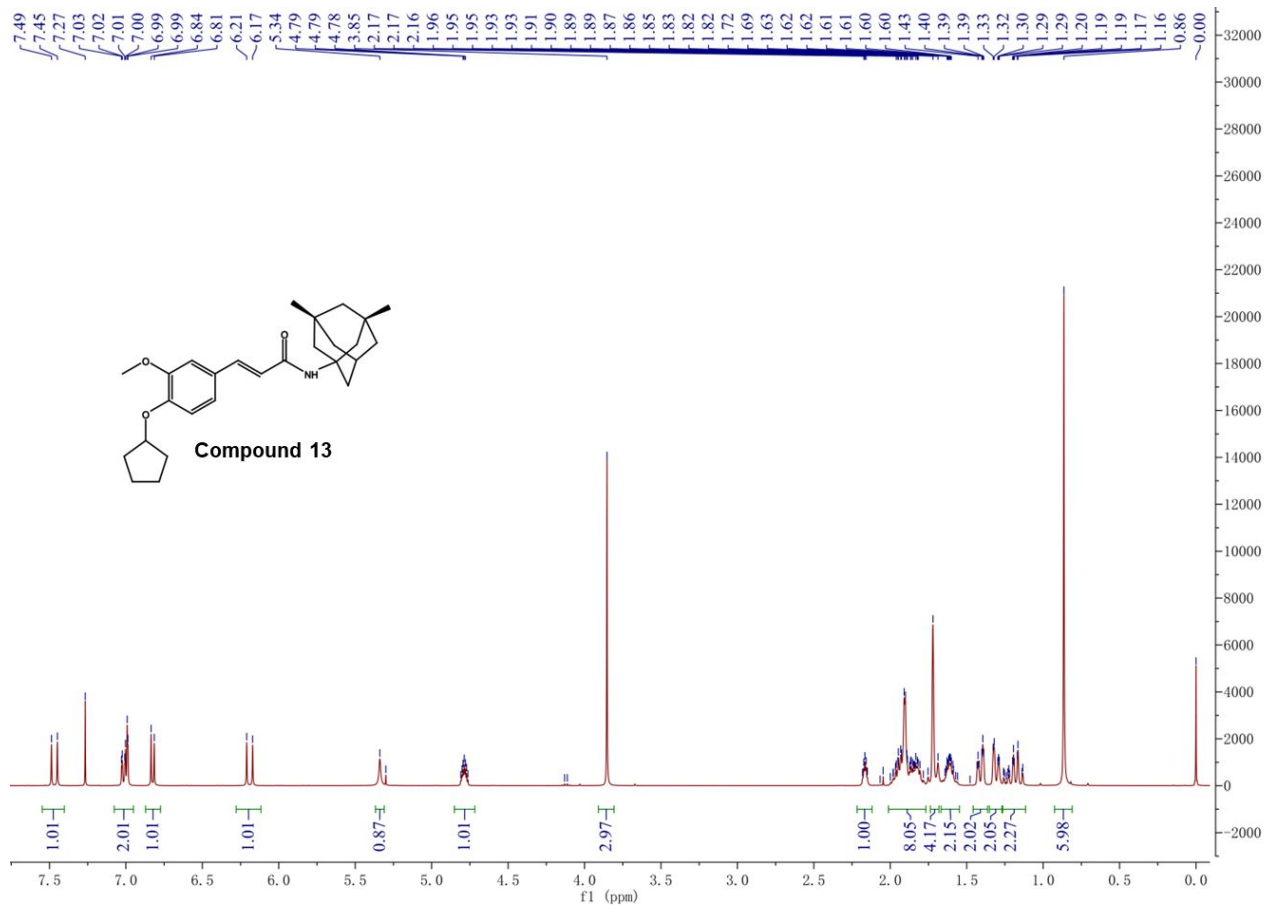
^{13}C NMR compound 11



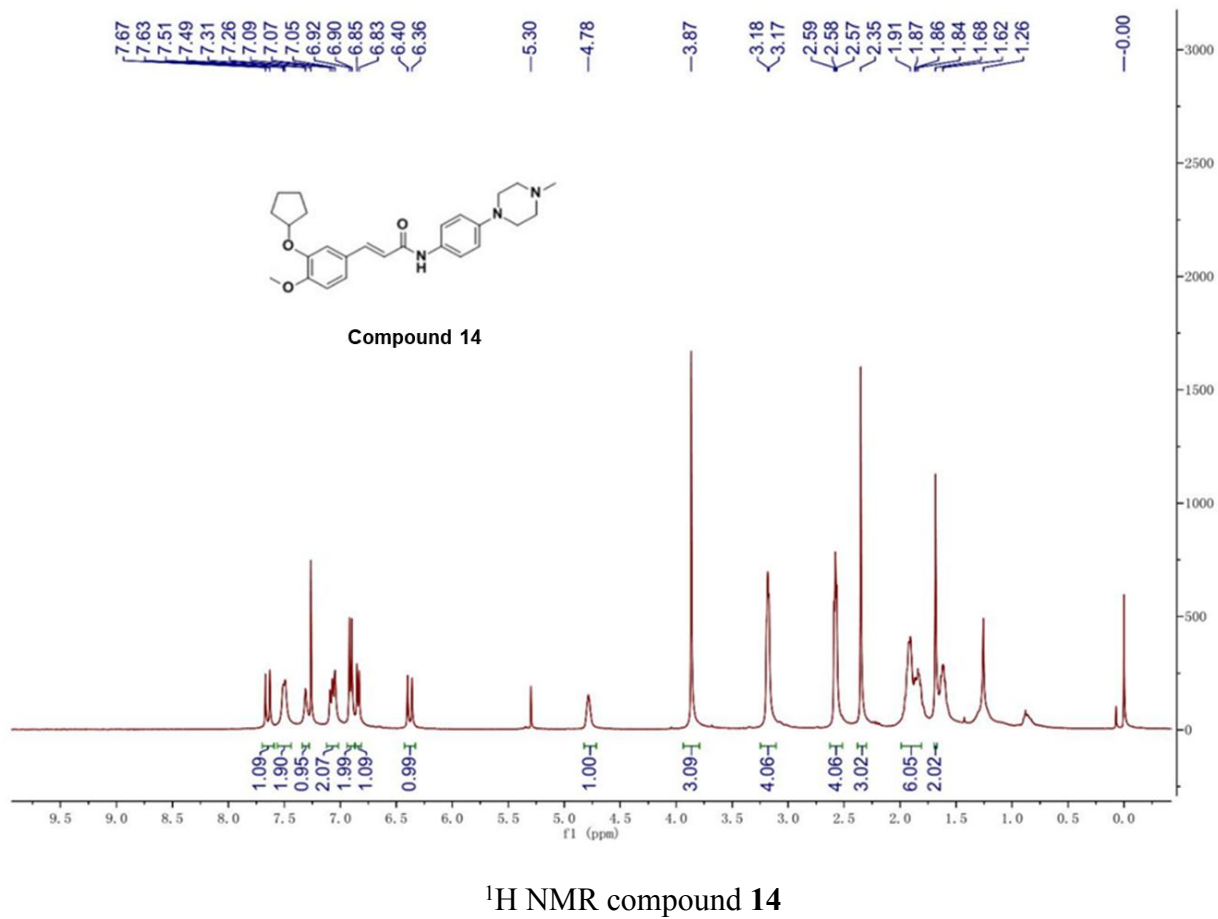
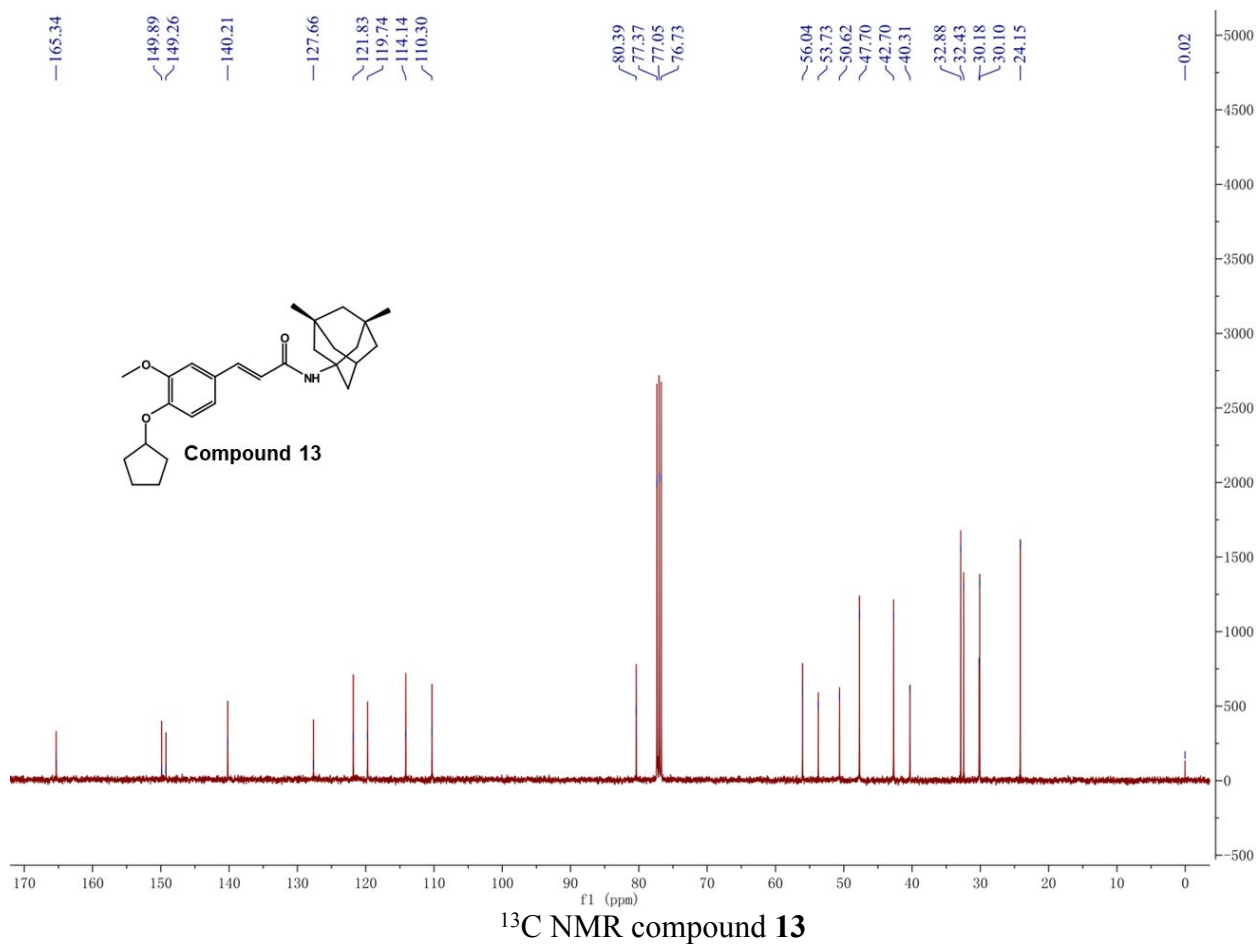
^1H NMR compound 12

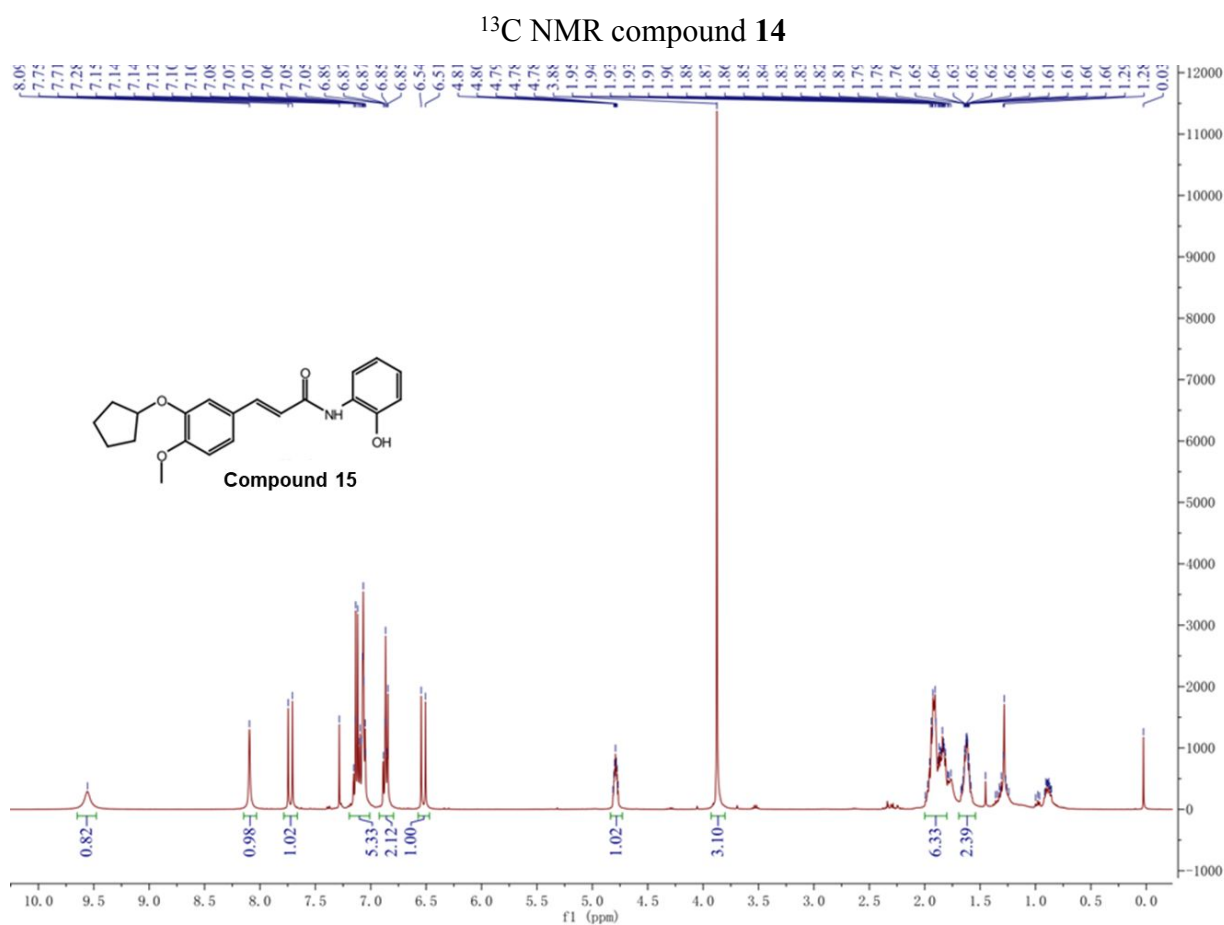
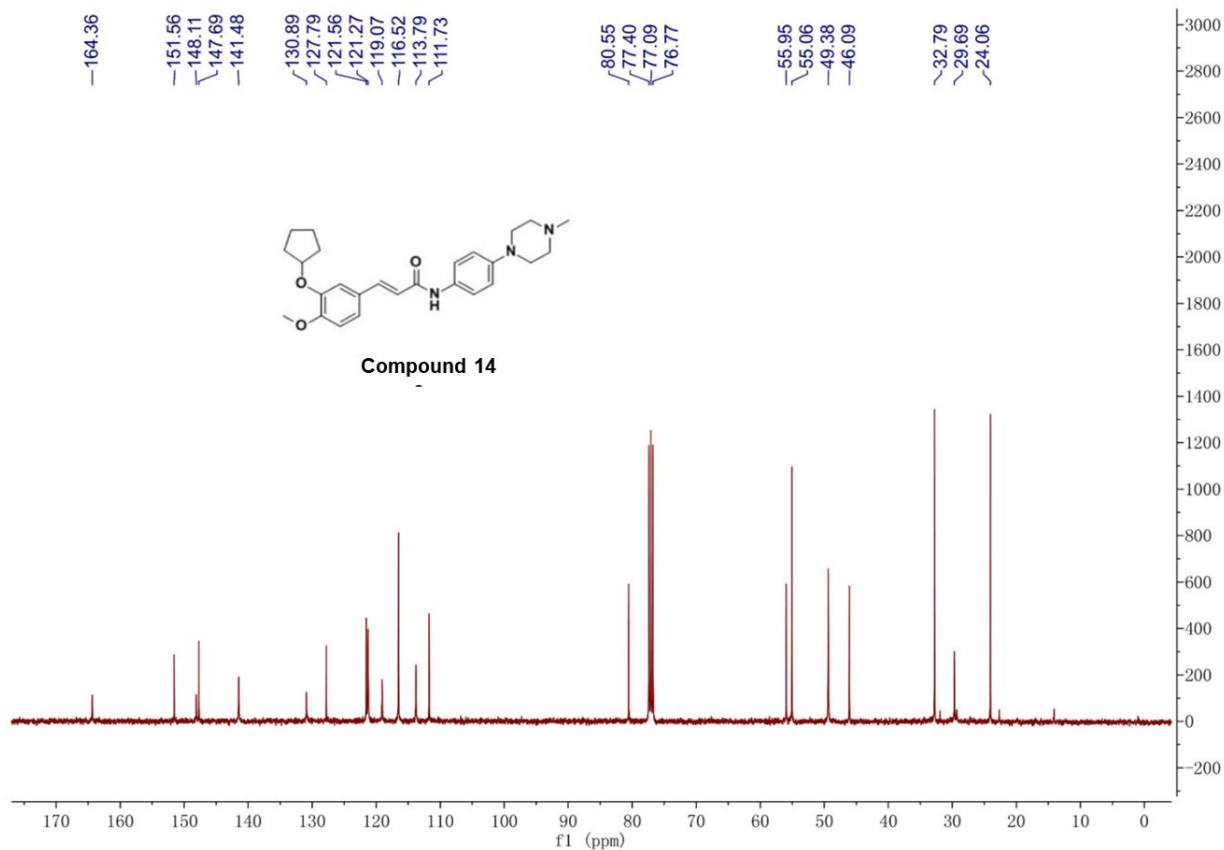


¹³C NMR compound 12

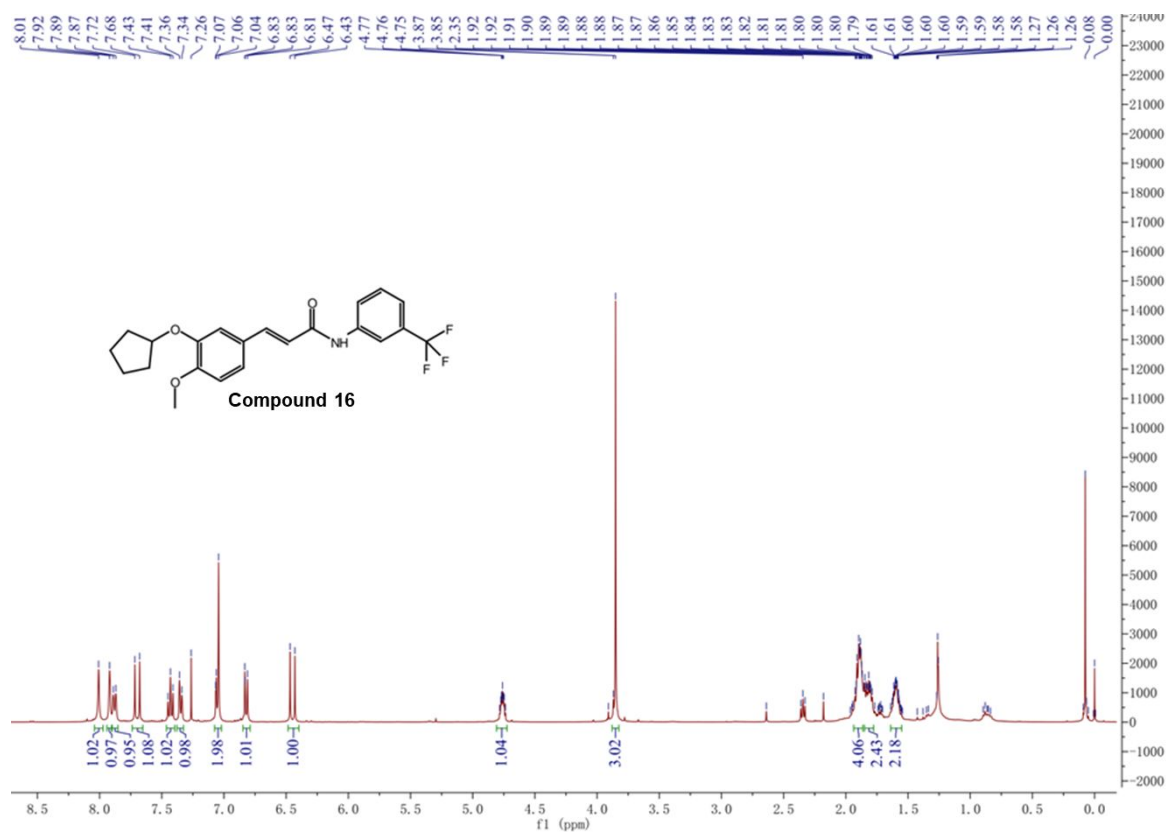
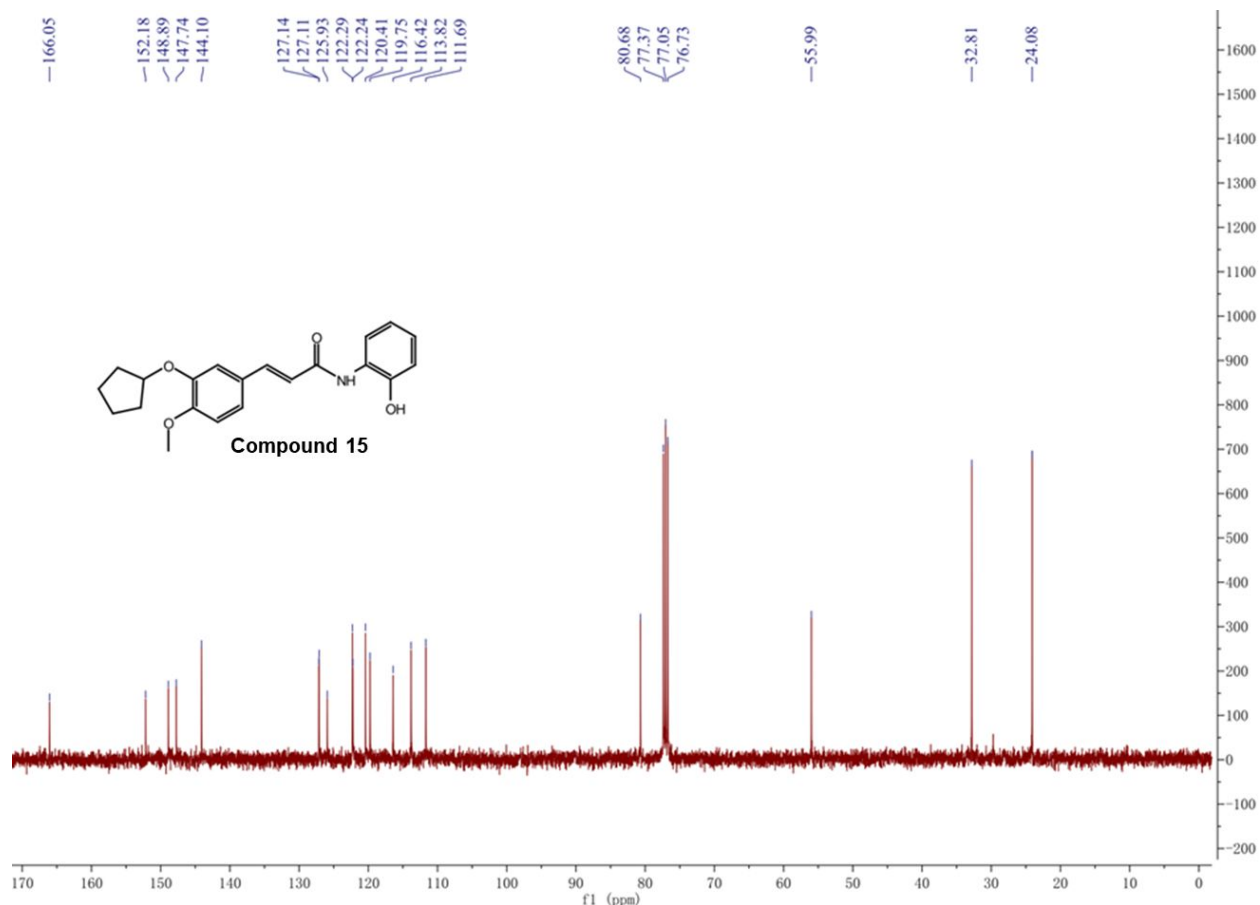


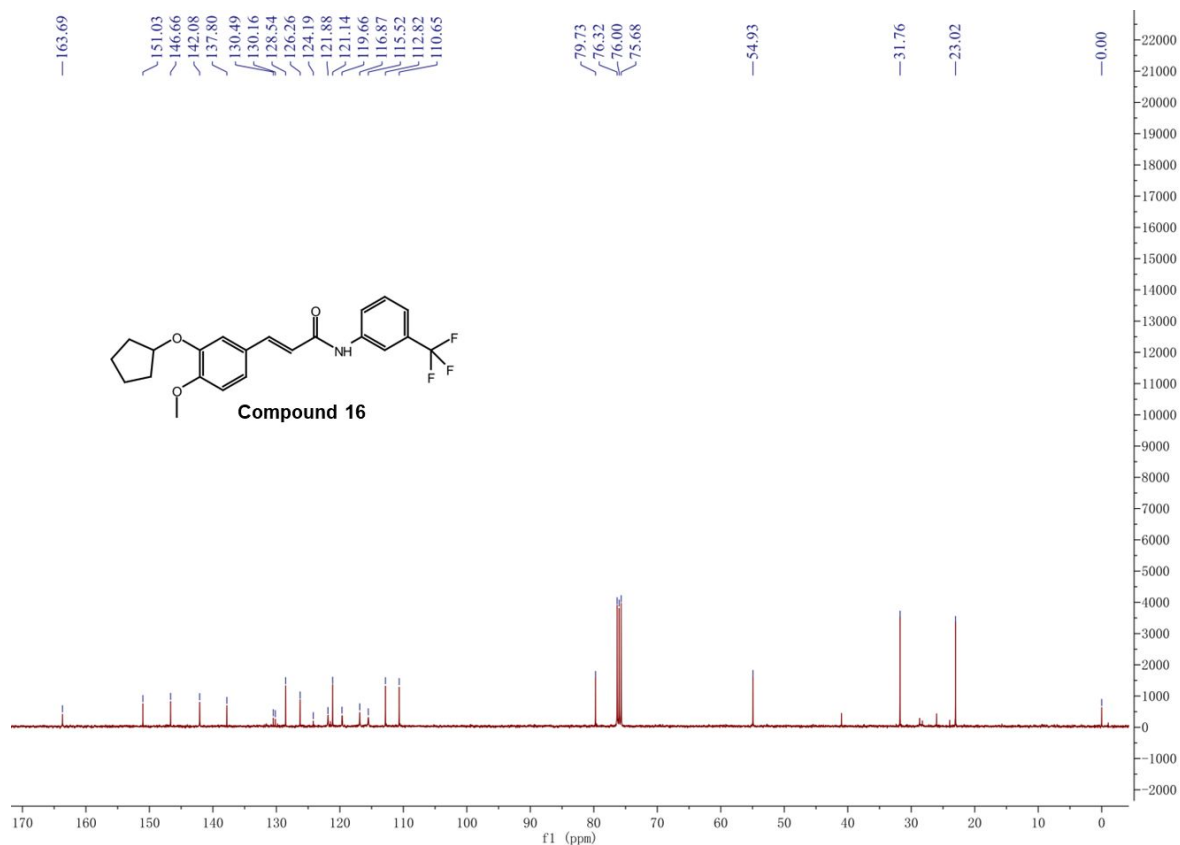
¹H NMR compound 13



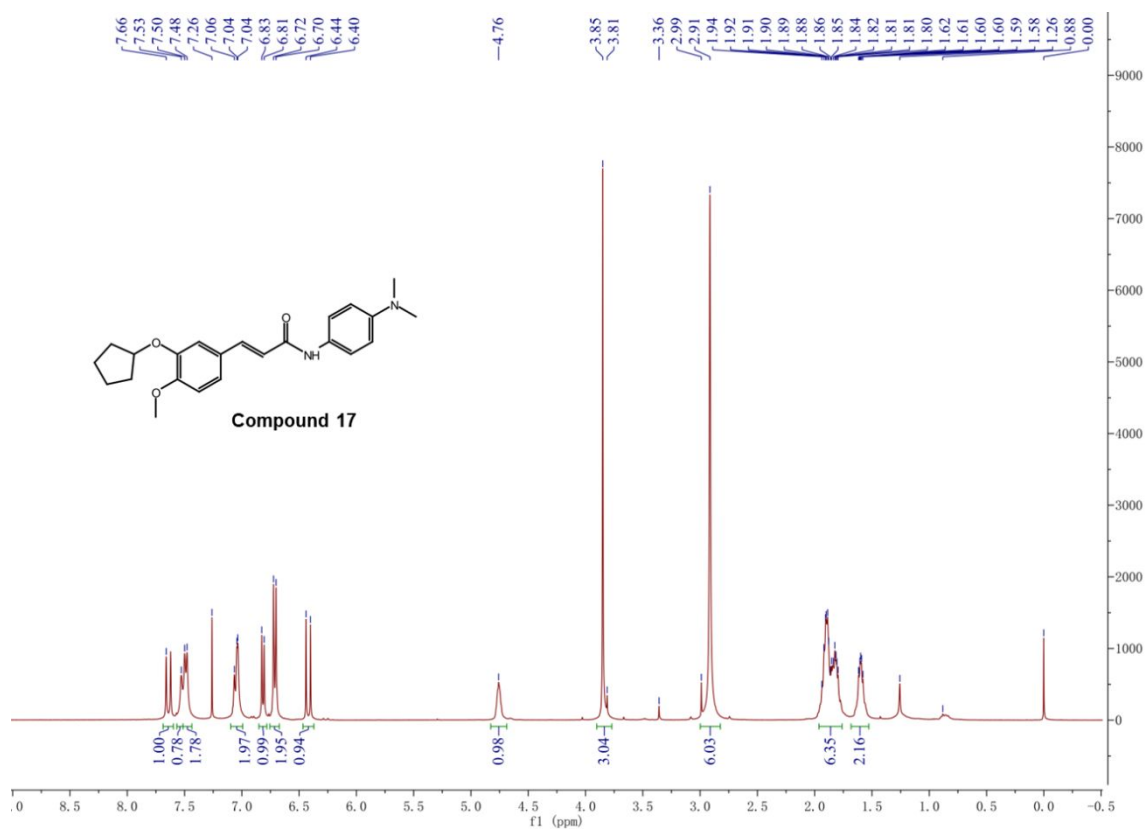


¹H NMR compound 15

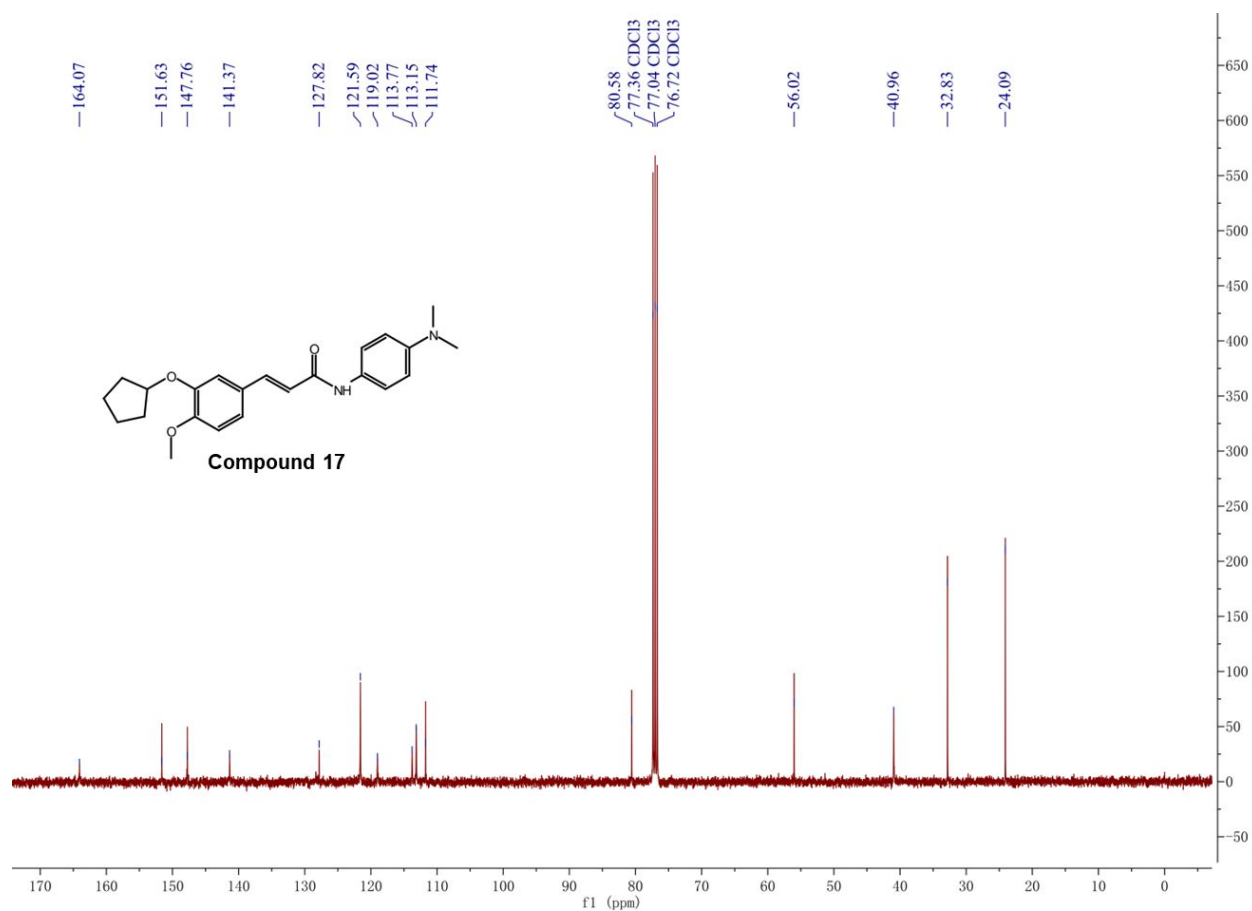




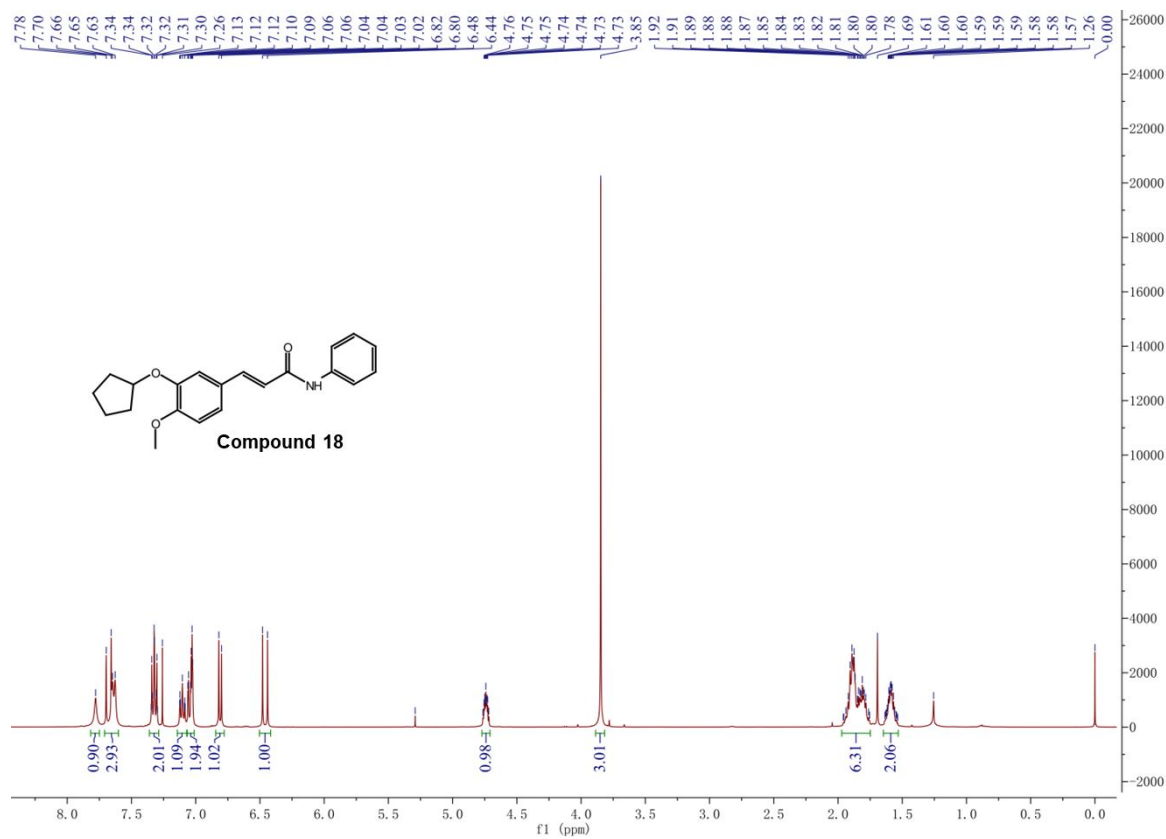
¹³C NMR compound 16



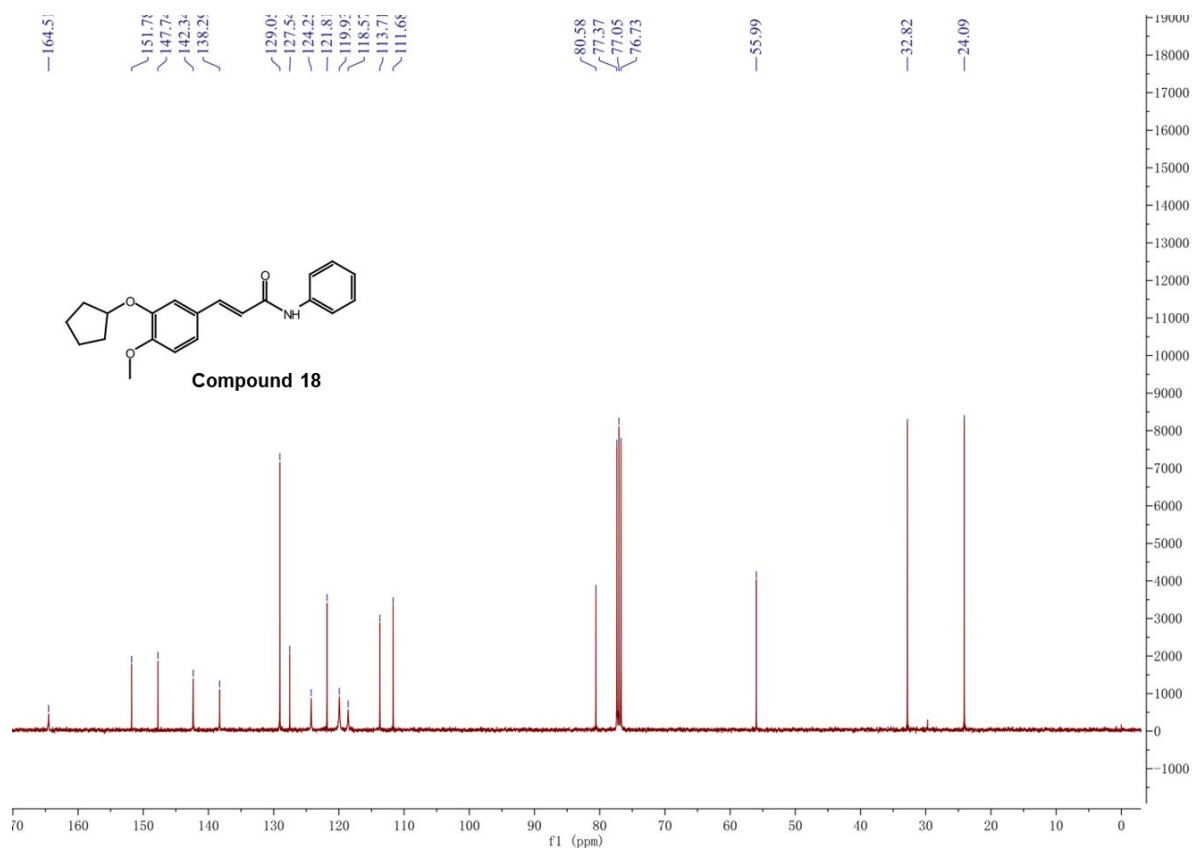
¹H NMR compound 17



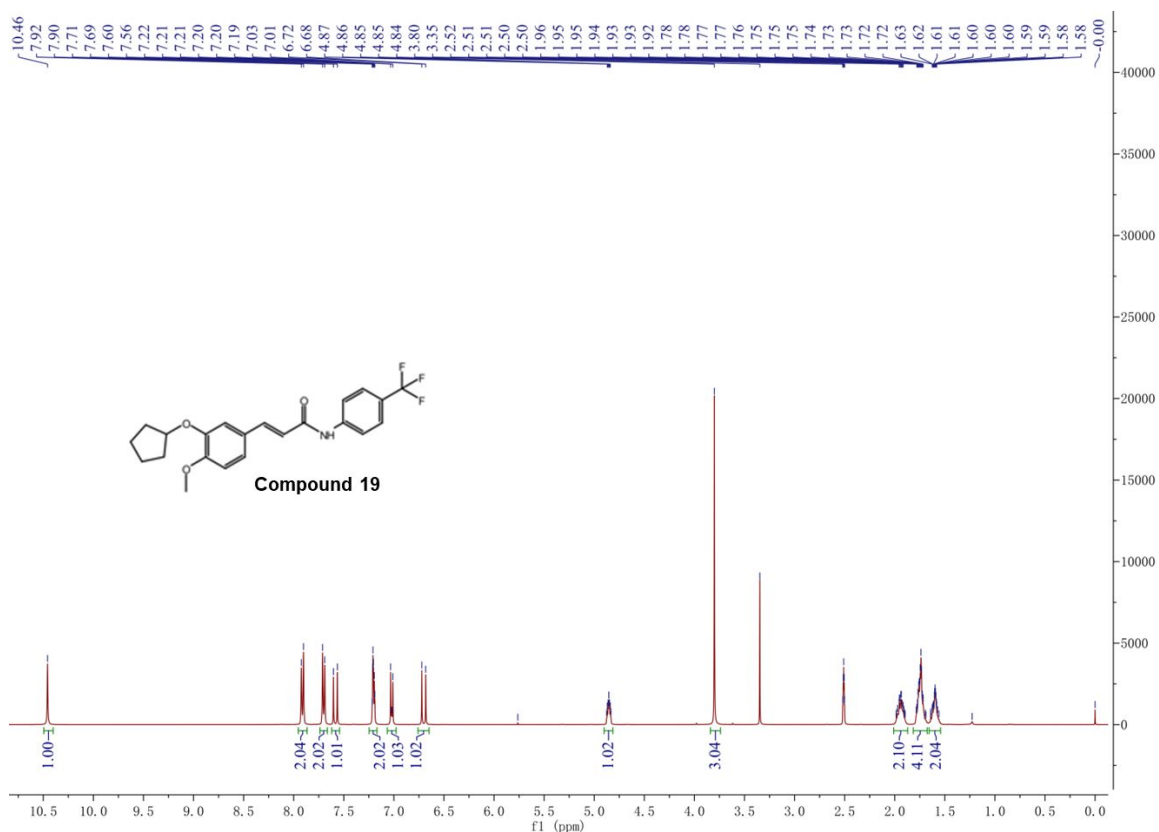
¹³C NMR compound 17



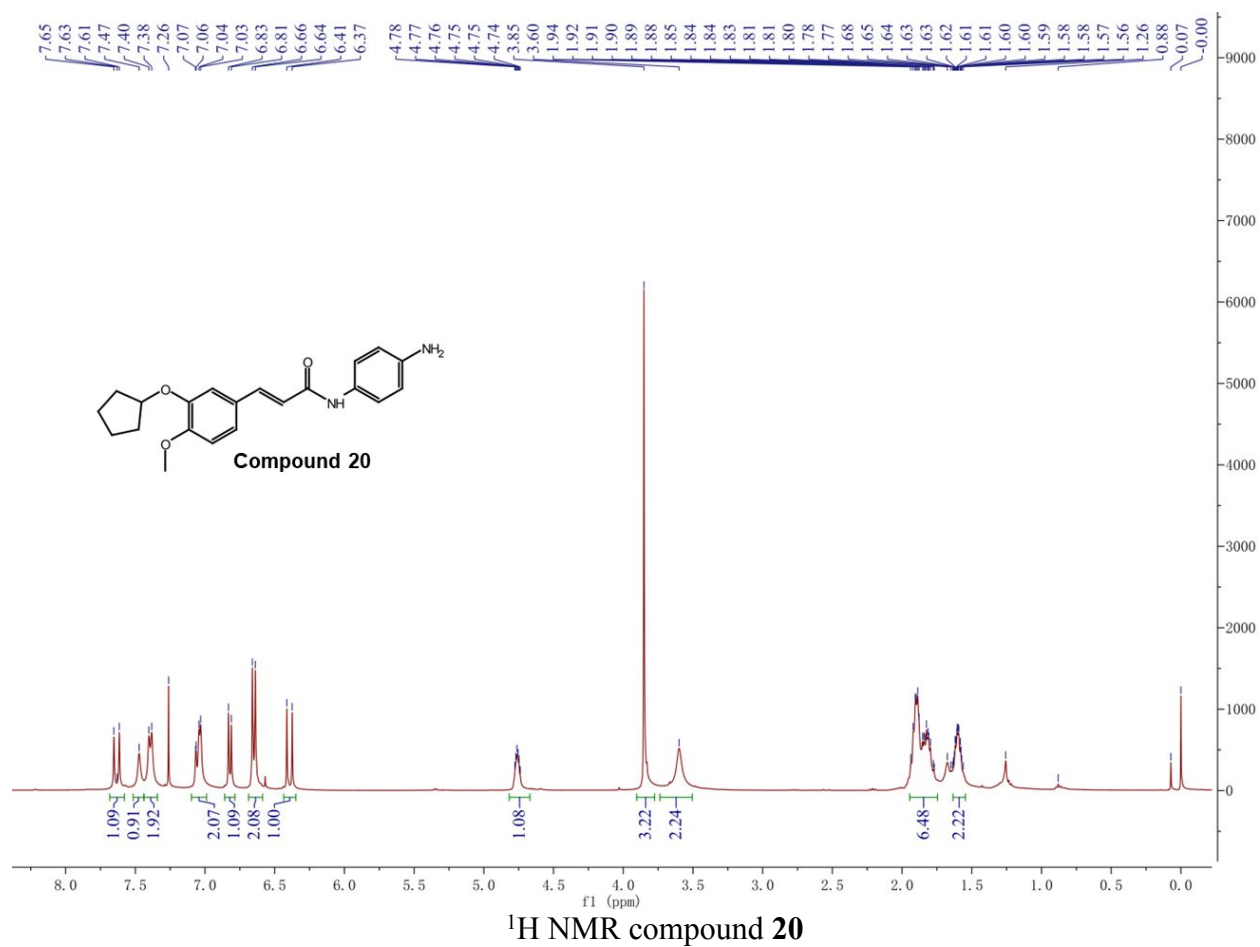
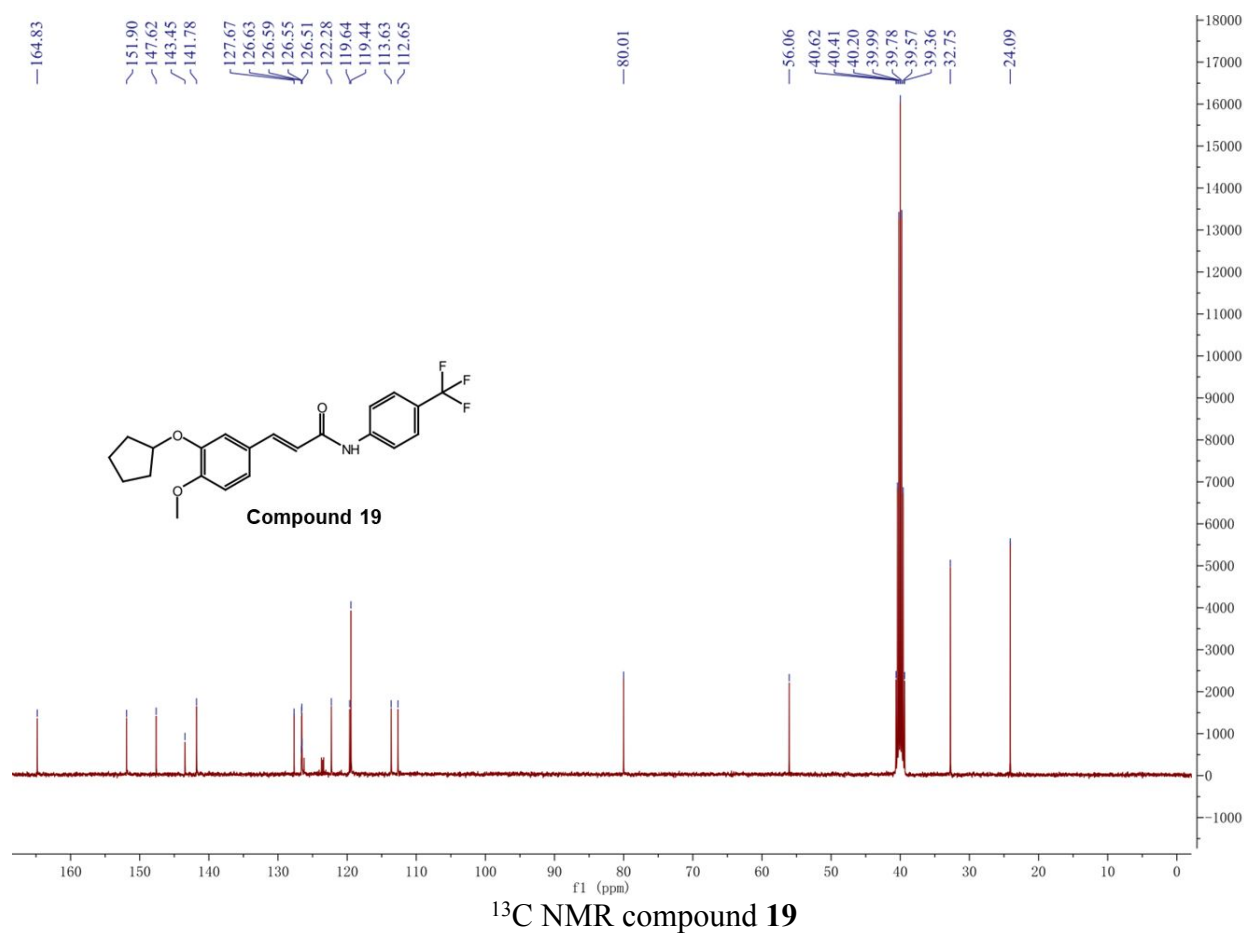
¹H NMR compound 18

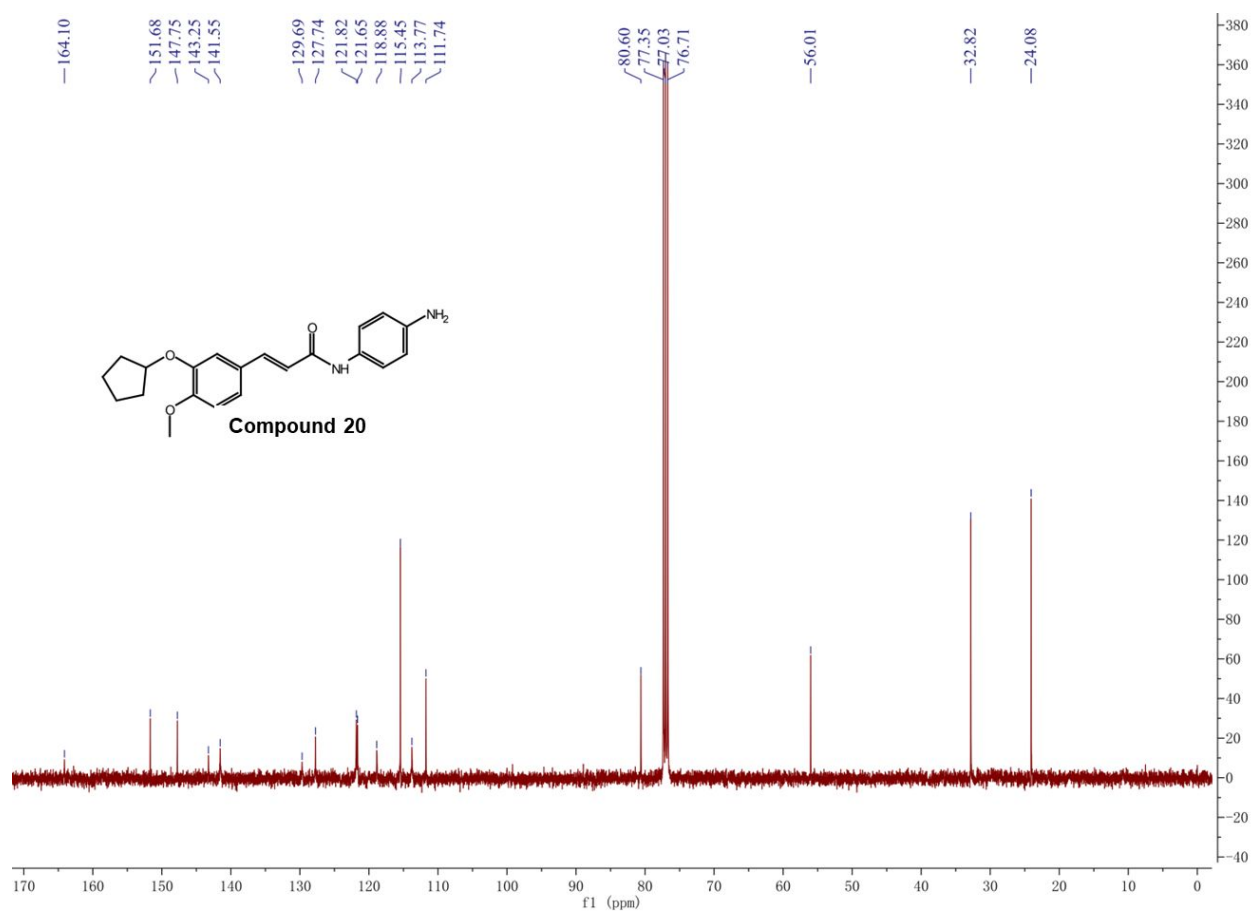


^{13}C NMR compound **18**

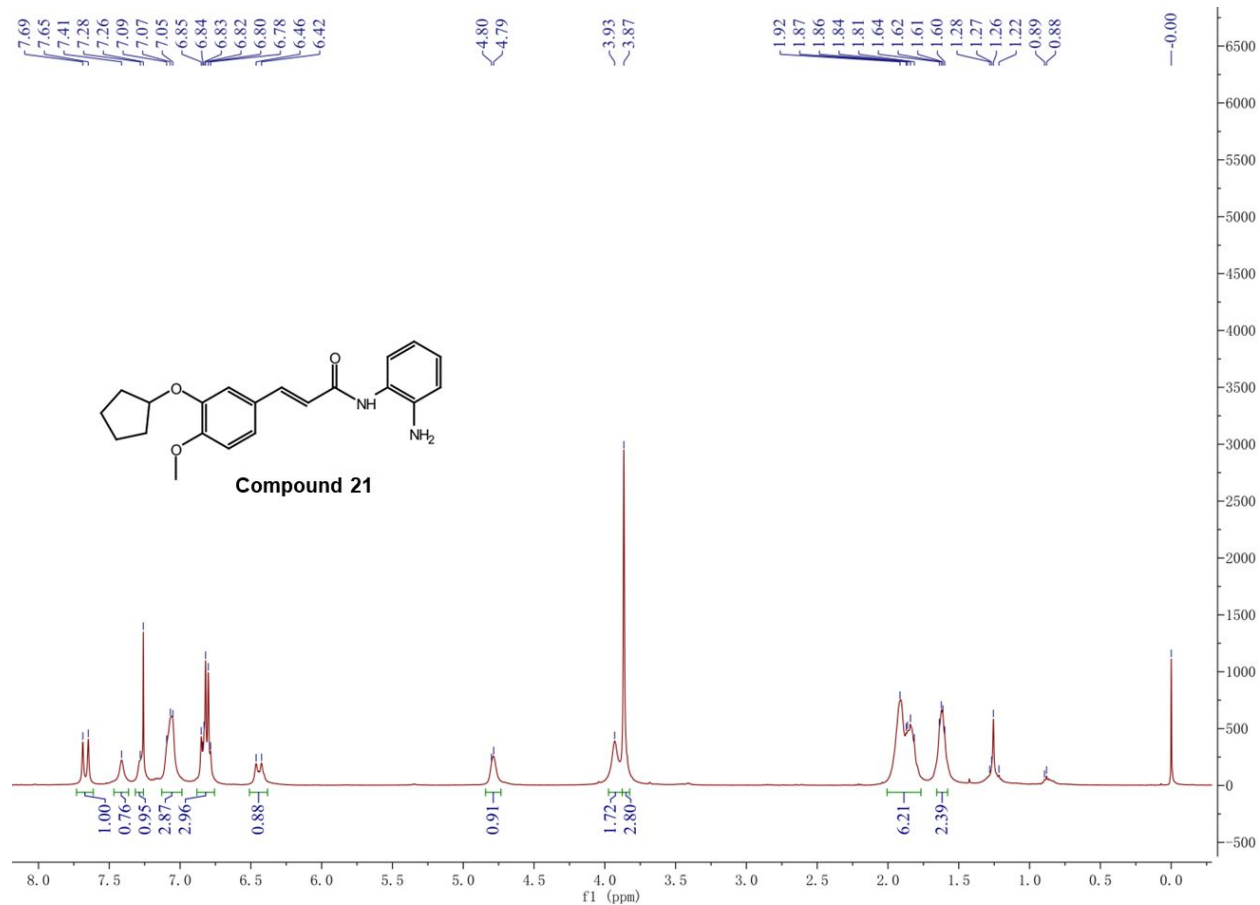


^1H NMR compound **19**

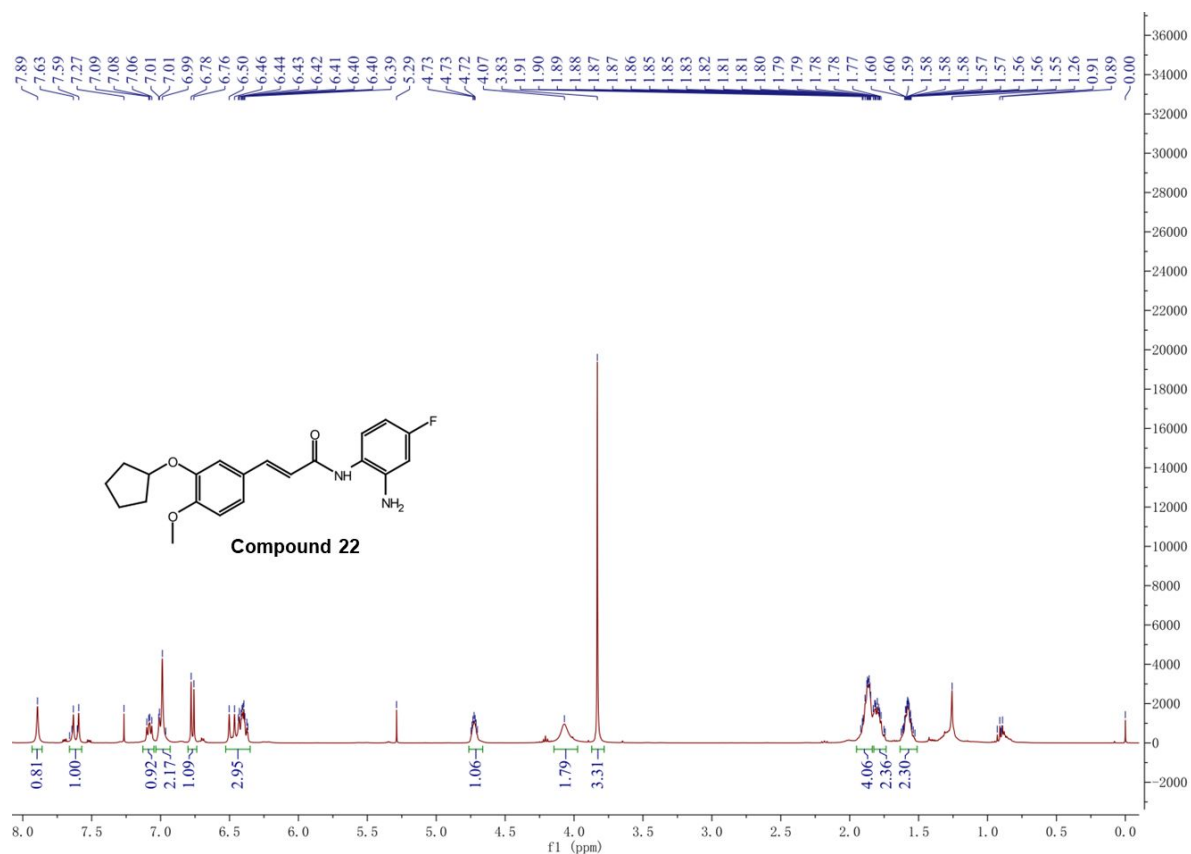
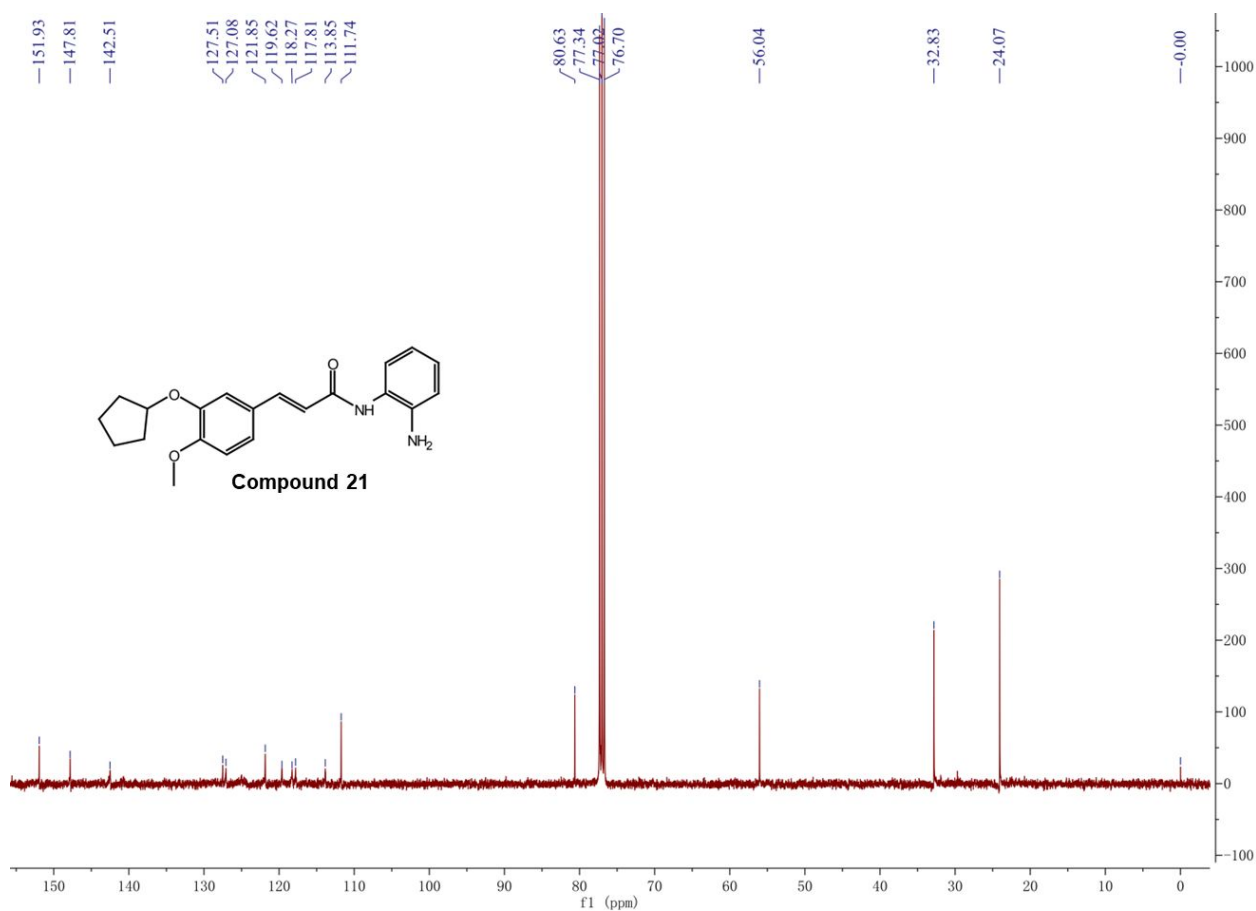


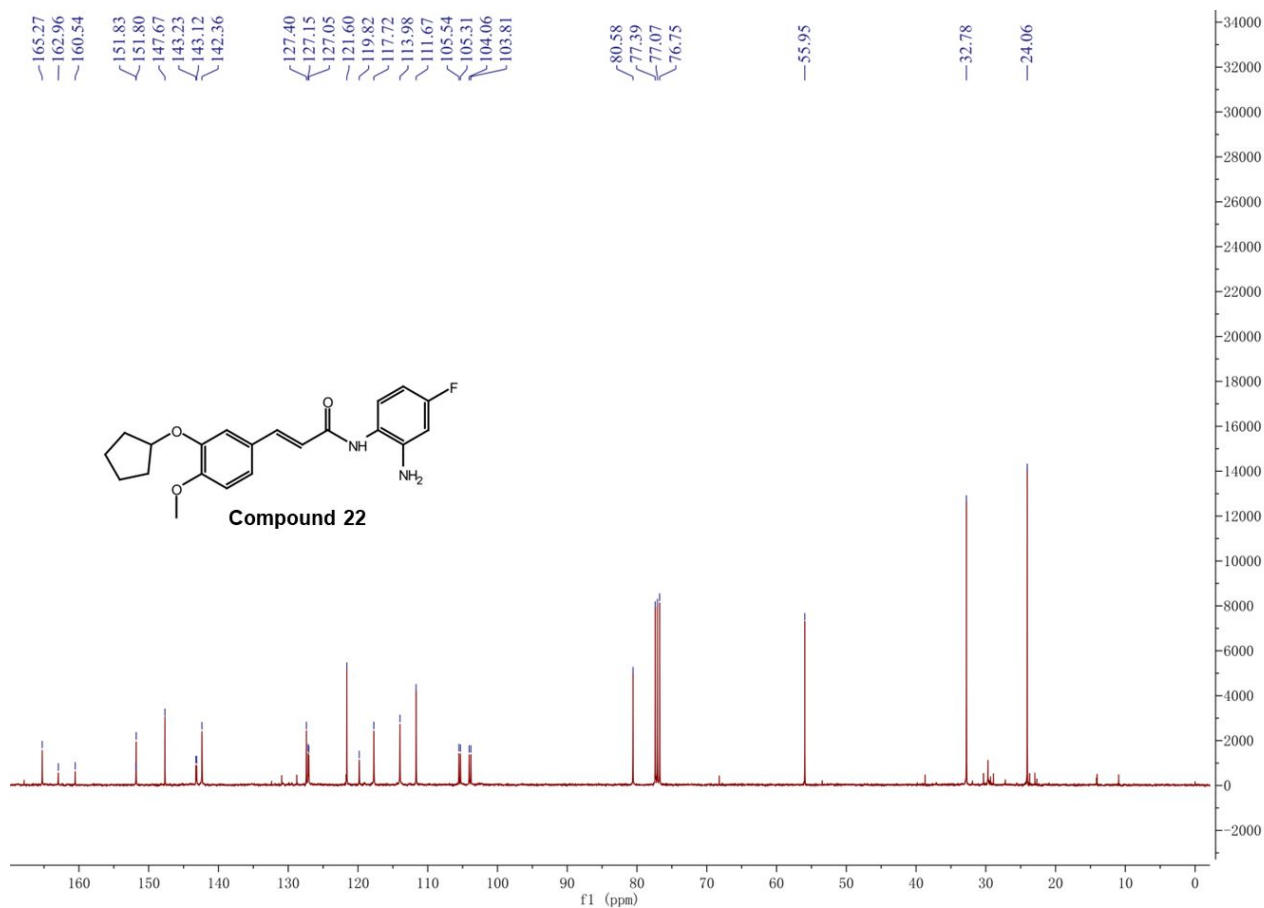


¹³C NMR compound 20

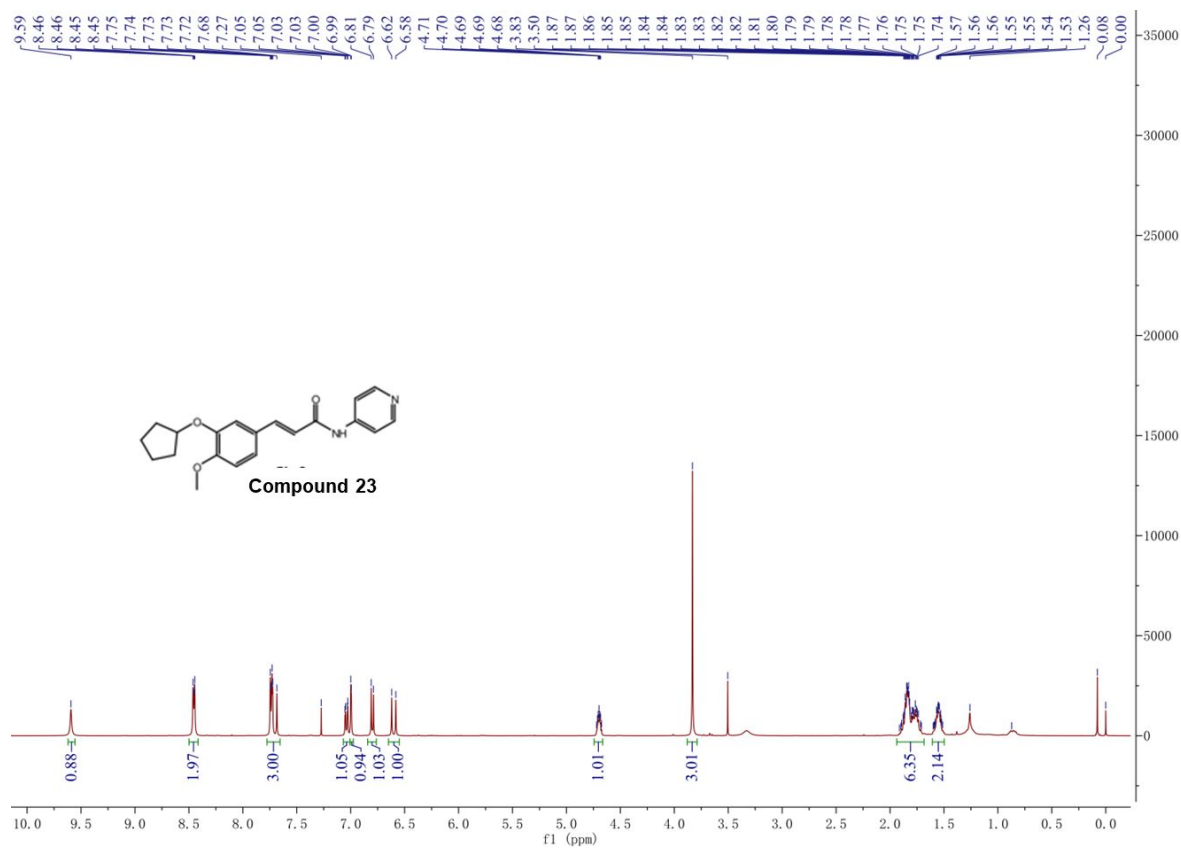


¹H NMR compound 21

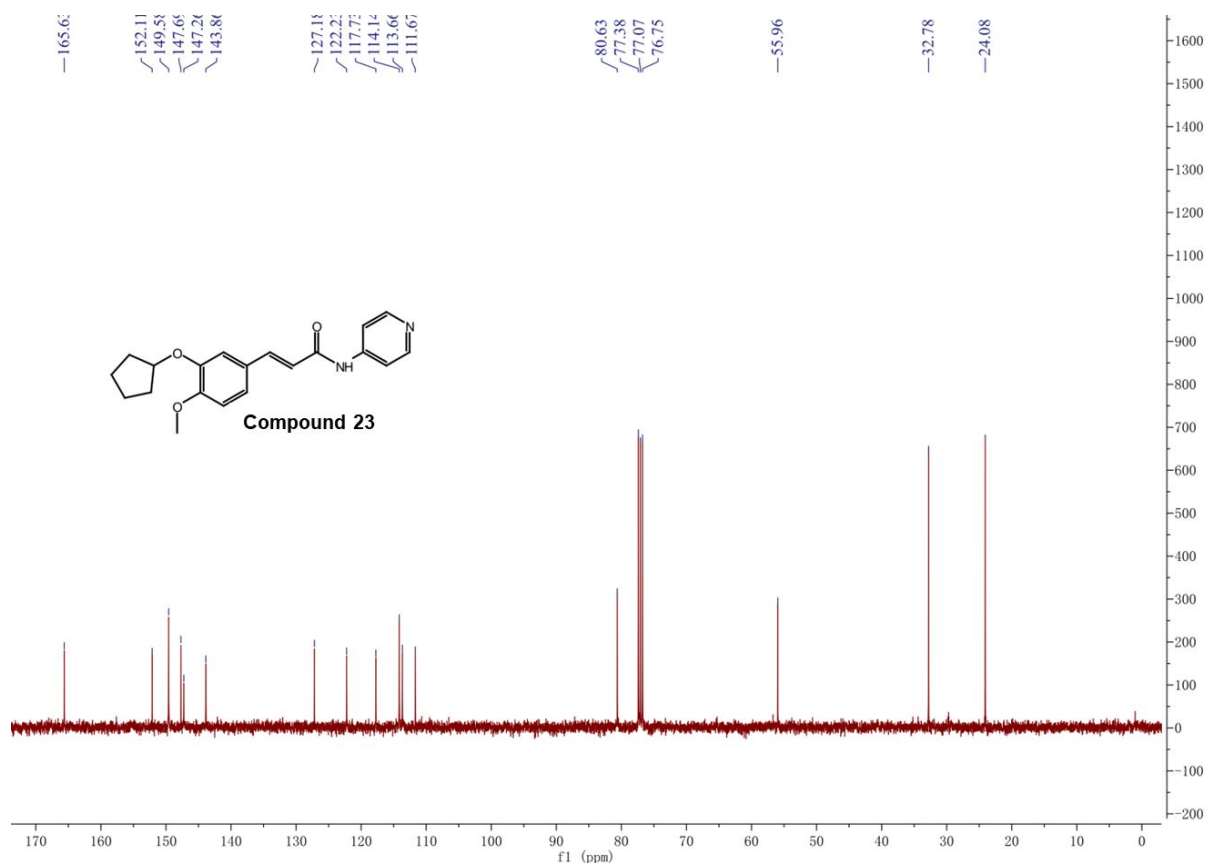




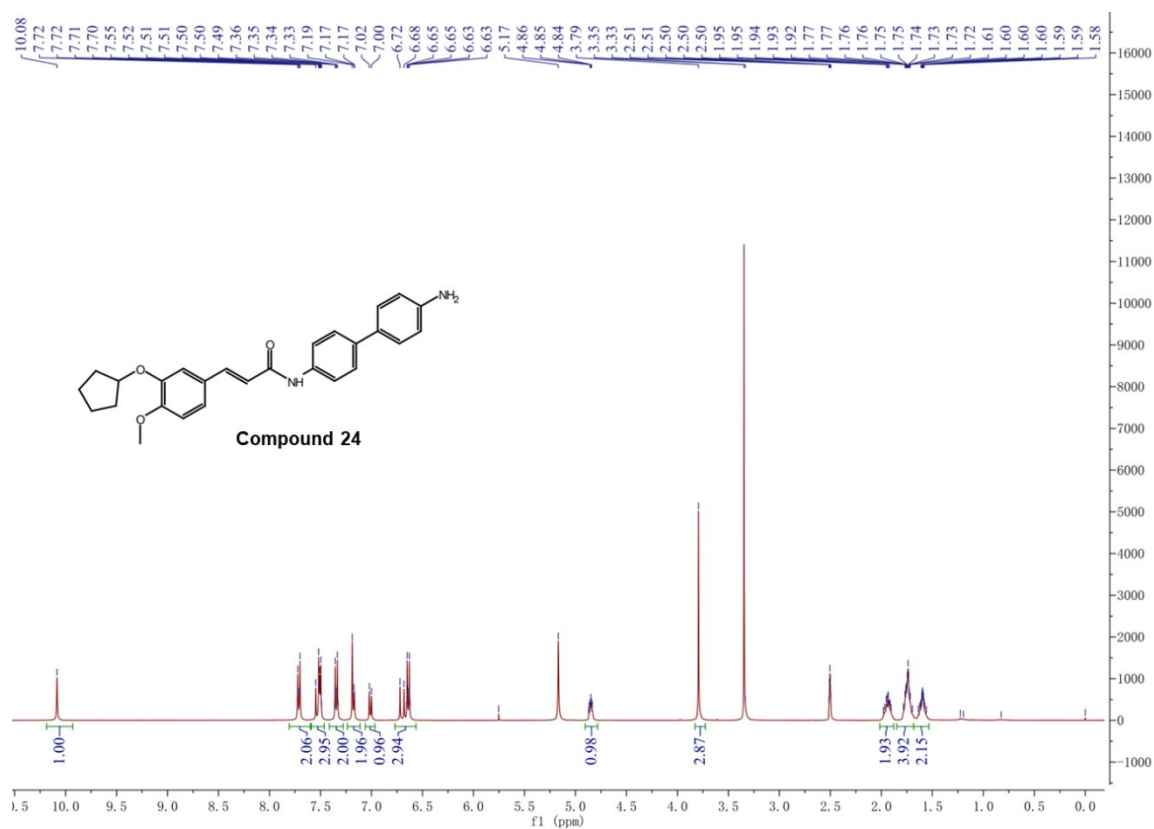
¹³C NMR compound 22



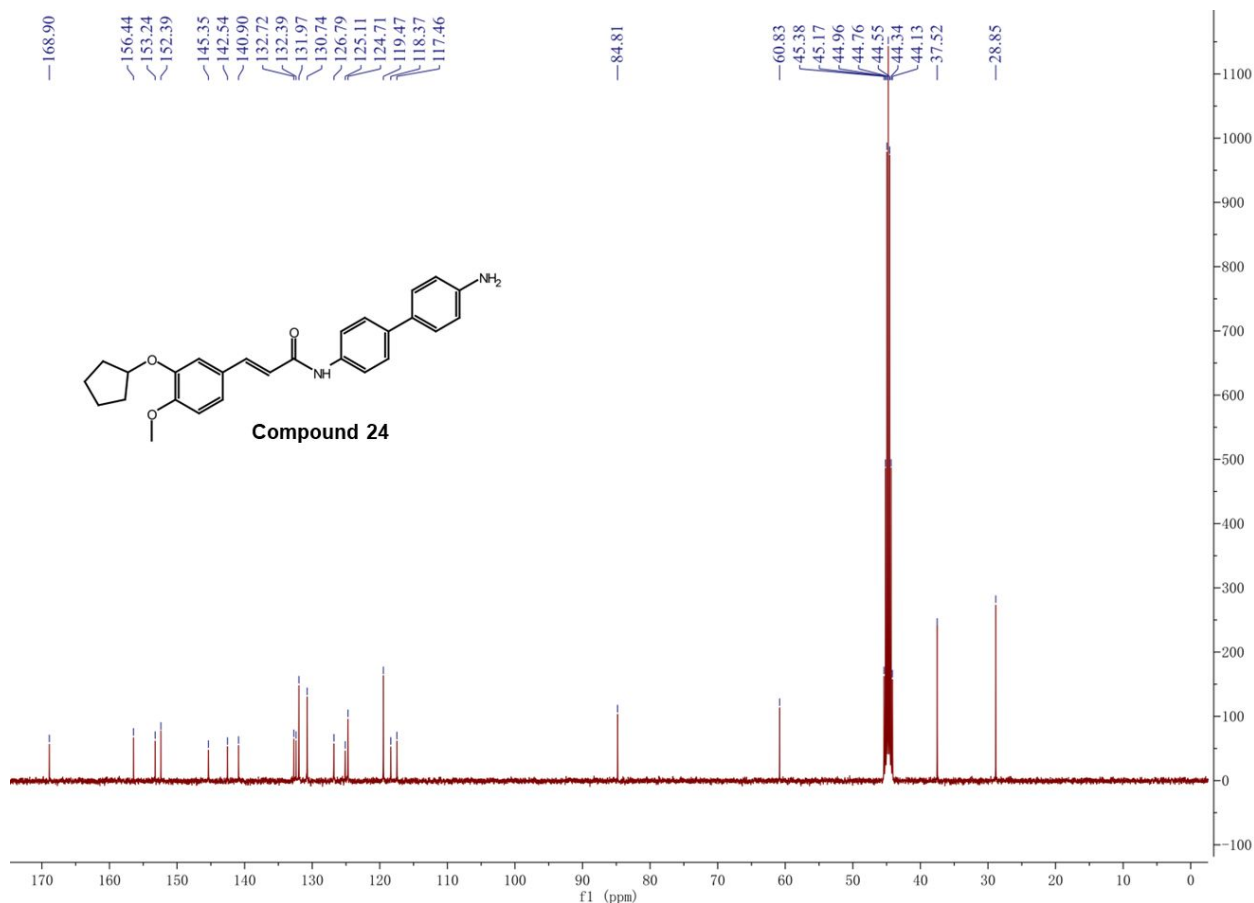
¹H NMR compound 23



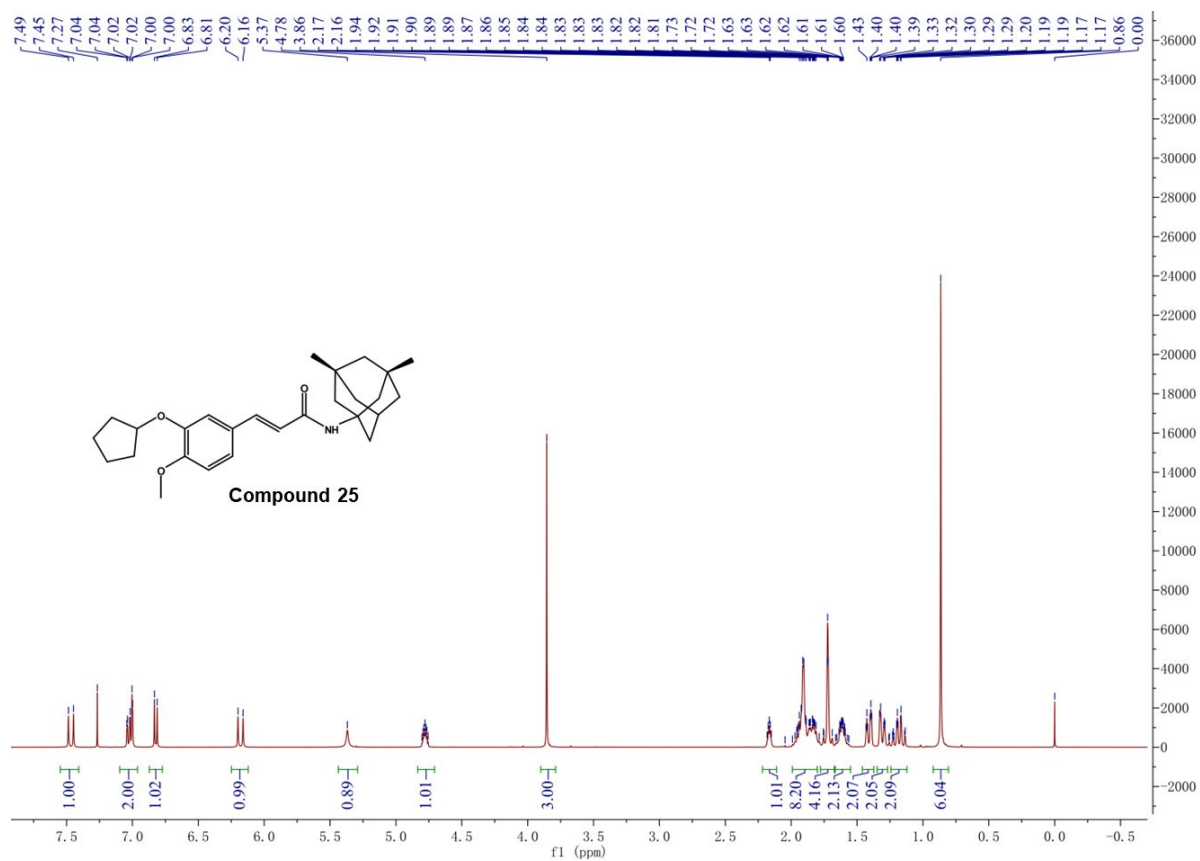
¹³C NMR compound 23



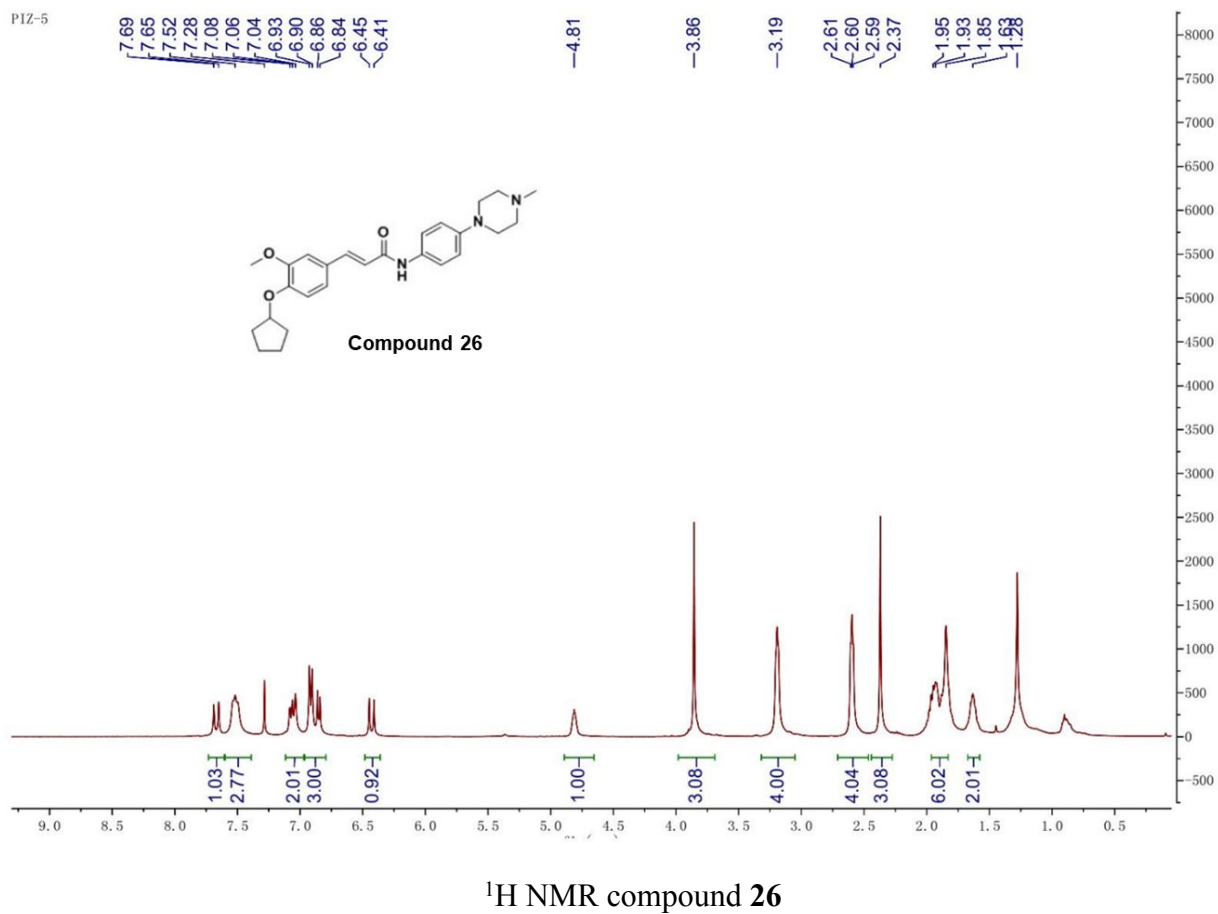
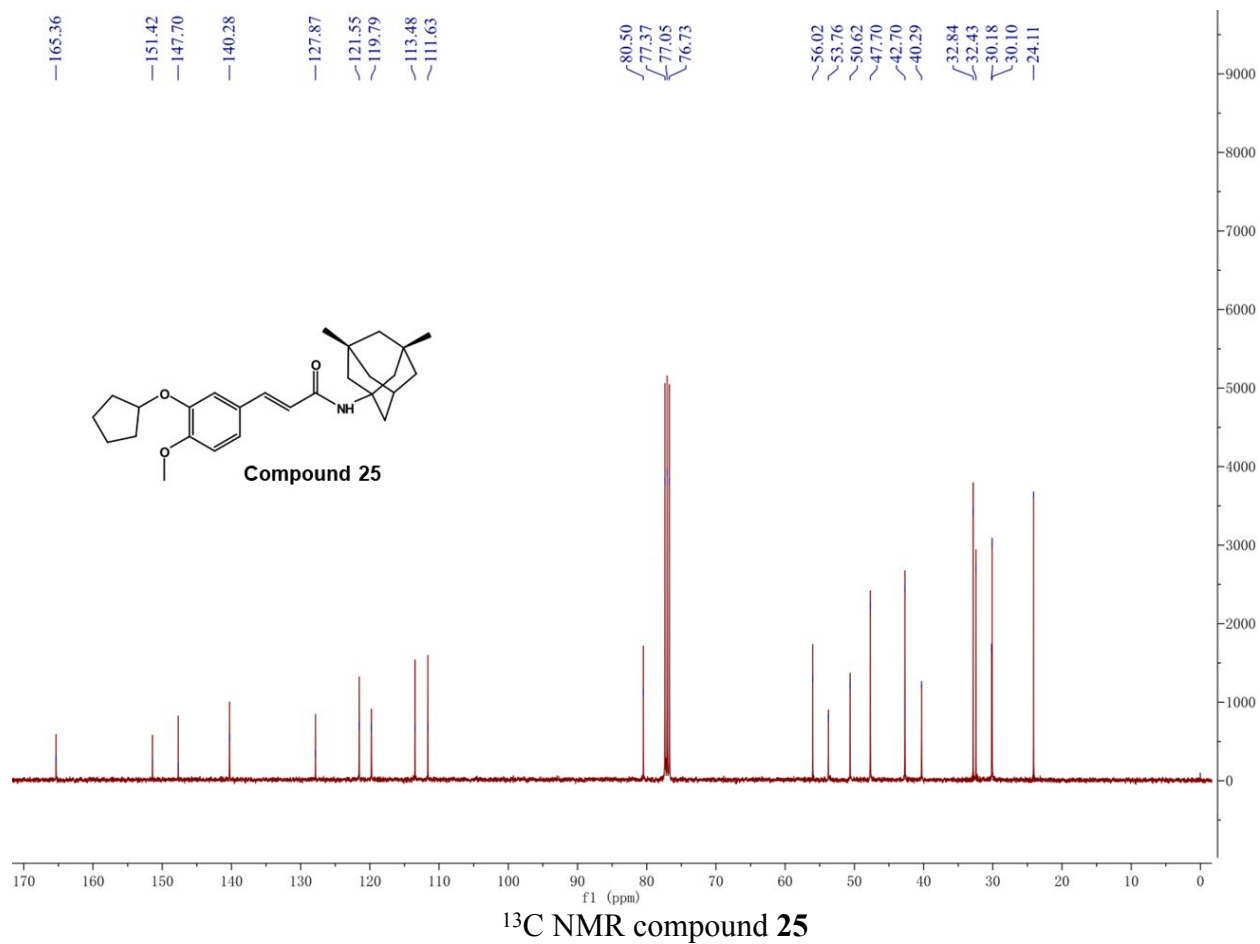
¹H NMR compound 24

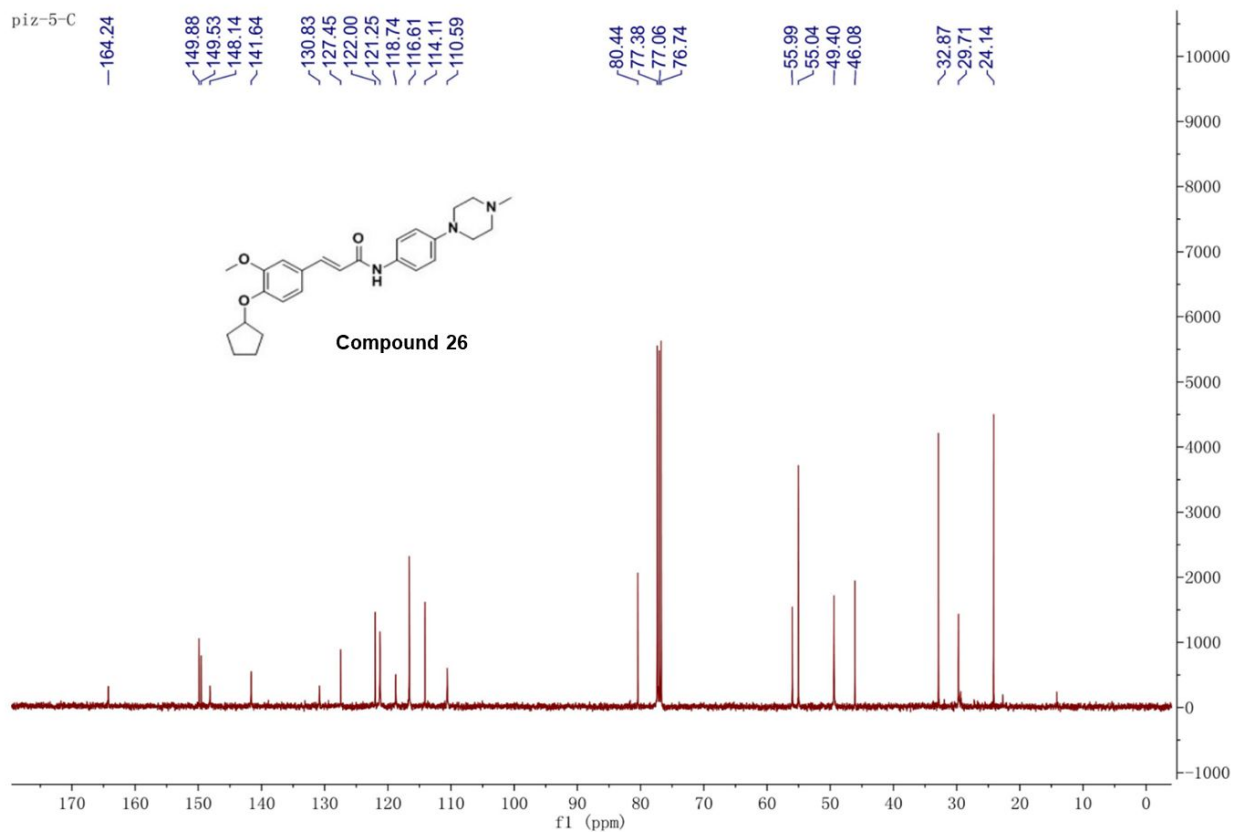


¹³C NMR compound 24



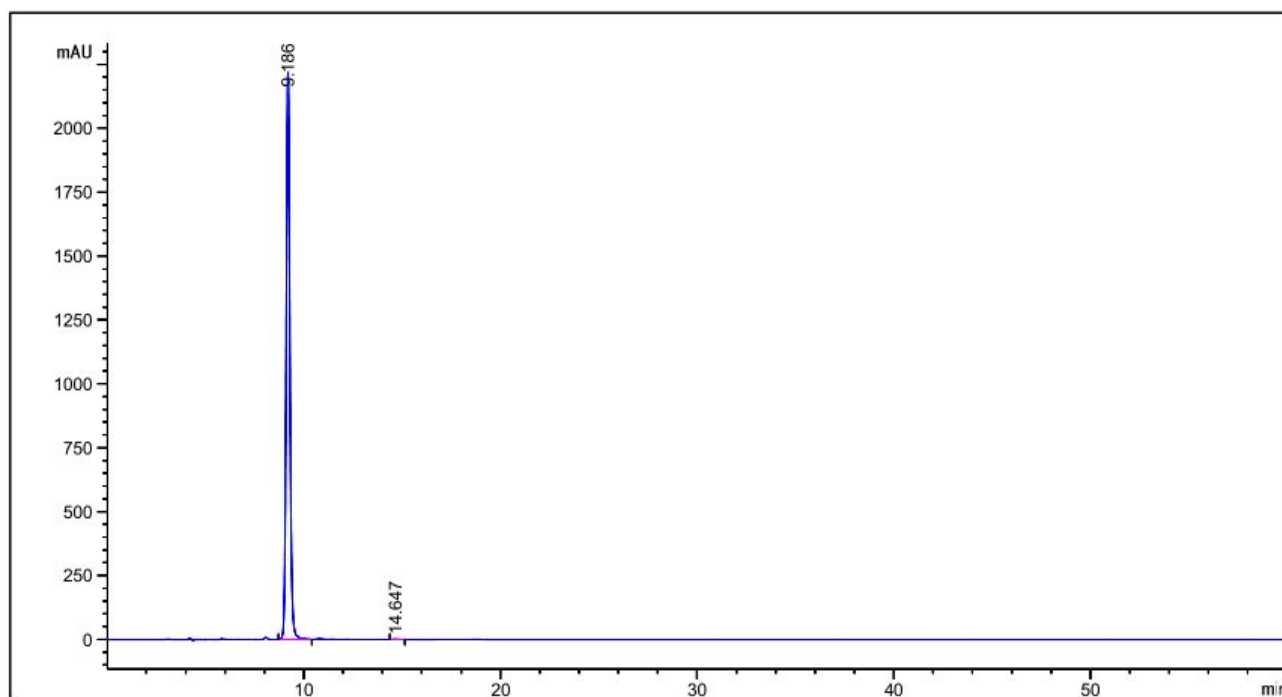
¹H NMR compound 25





^{13}C NMR compound **26**

HPLC of the compound 5



面积百分比报告

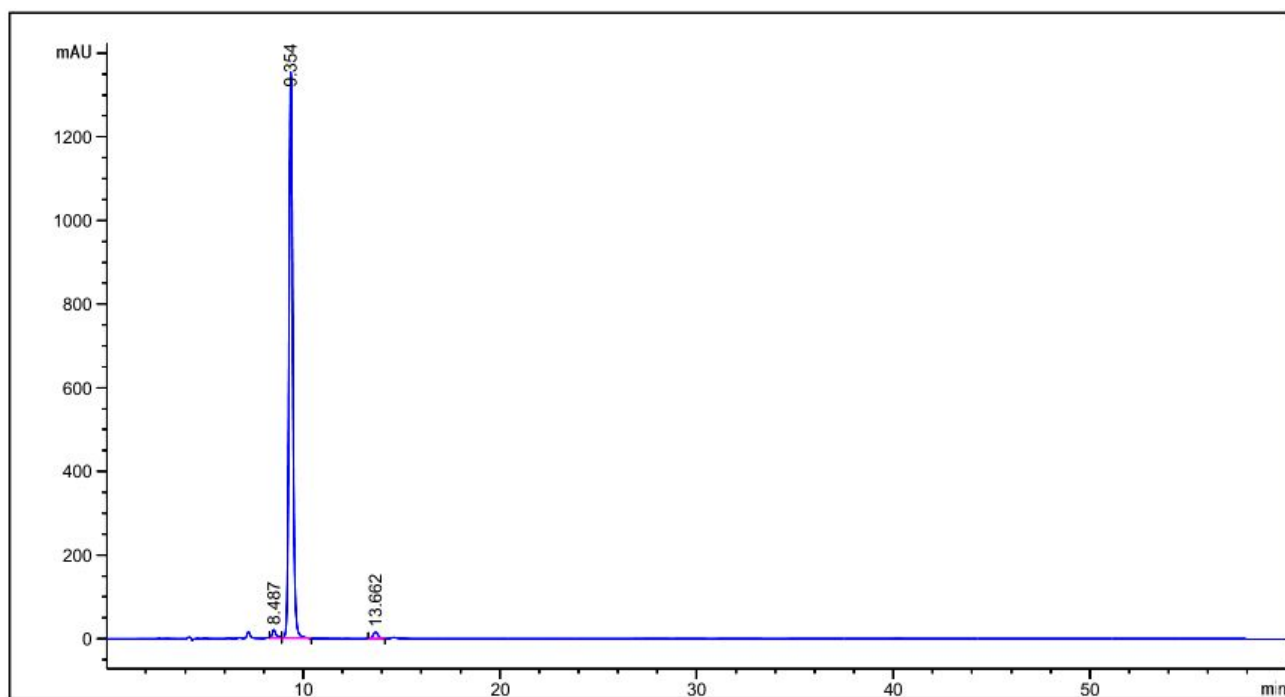
排序 : 信号
乘积因子 : 1.0000
稀释因子 : 1.0000
内标使用乘积因子和稀释因子

信号 1: DAD1 B, Sig=245,8 Ref=600,100

峰 #	保留时间 [min]	类型	峰宽 [min]	峰面积 [mAU*s]	峰高 [mAU]	峰面积 %
1	9.186	BB	0.1995	2.88478e4	2221.28101	99.9197
2	14.647	BB	0.2889	23.18740	1.24707	0.0803

总量 : 2.88709e4 2222.52808

HPLC of the compound 6



面积百分比报告

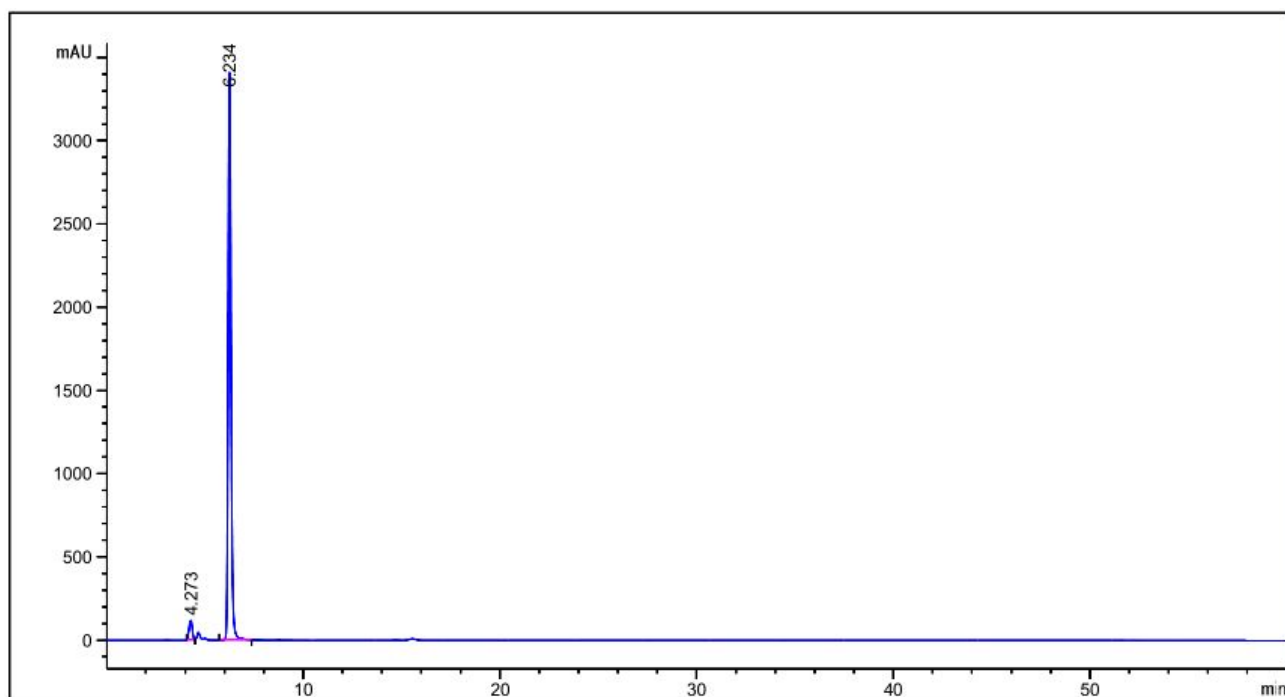
排序 : 信号
乘积因子 : 1.0000
稀释因子 : 1.0000
内标使用乘积因子和稀释因子

信号 1: DAD1 B, Sig=245,8 Ref=600,100

峰 #	保留时间 [min]	类型	峰宽 [min]	峰面积 [mAU*s]	峰高 [mAU]	峰面积 %
1	8.487	VV	0.2219	318.17203	20.86035	1.6928
2	9.354	VB	0.2066	1.81929e4	1354.97571	96.7911
3	13.662	BB	0.2875	284.97760	15.28587	1.5162

总量 : 1.87961e4 1391.12193

HPLC of the compound 8



面积百分比报告

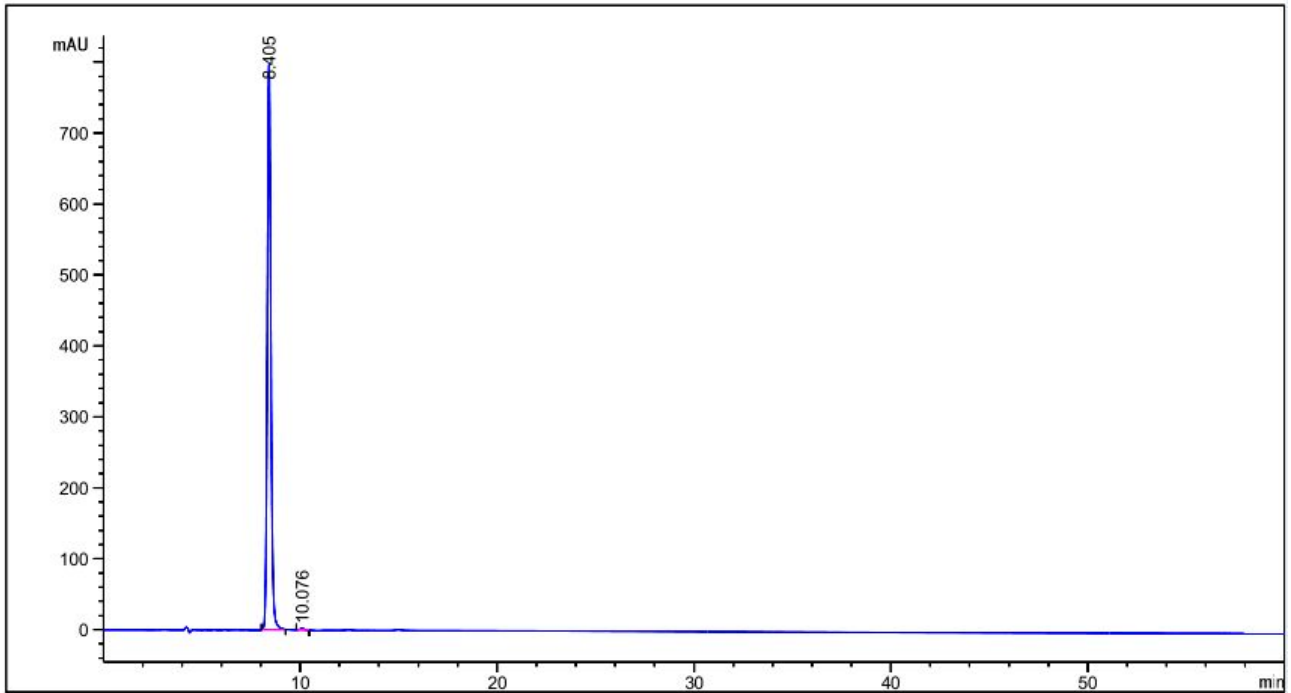
排序 : 信号
乘积因子 : 1.0000
稀释因子 : 1.0000
内标使用乘积因子和稀释因子

信号 1: DAD1 B, Sig=245,8 Ref=600,100

峰 #	保留时间 [min]	类型	峰宽 [min]	峰面积 [mAU*s]	峰高 [mAU]	峰面积 %
1	4.273	BV	0.1878	1418.50964	118.34002	3.9090
2	6.234	BB	0.1571	3.48701e4	3415.00879	96.0910

总量 : 3.62886e4 3533.34881

HPLC of the compound 12



面积百分比报告

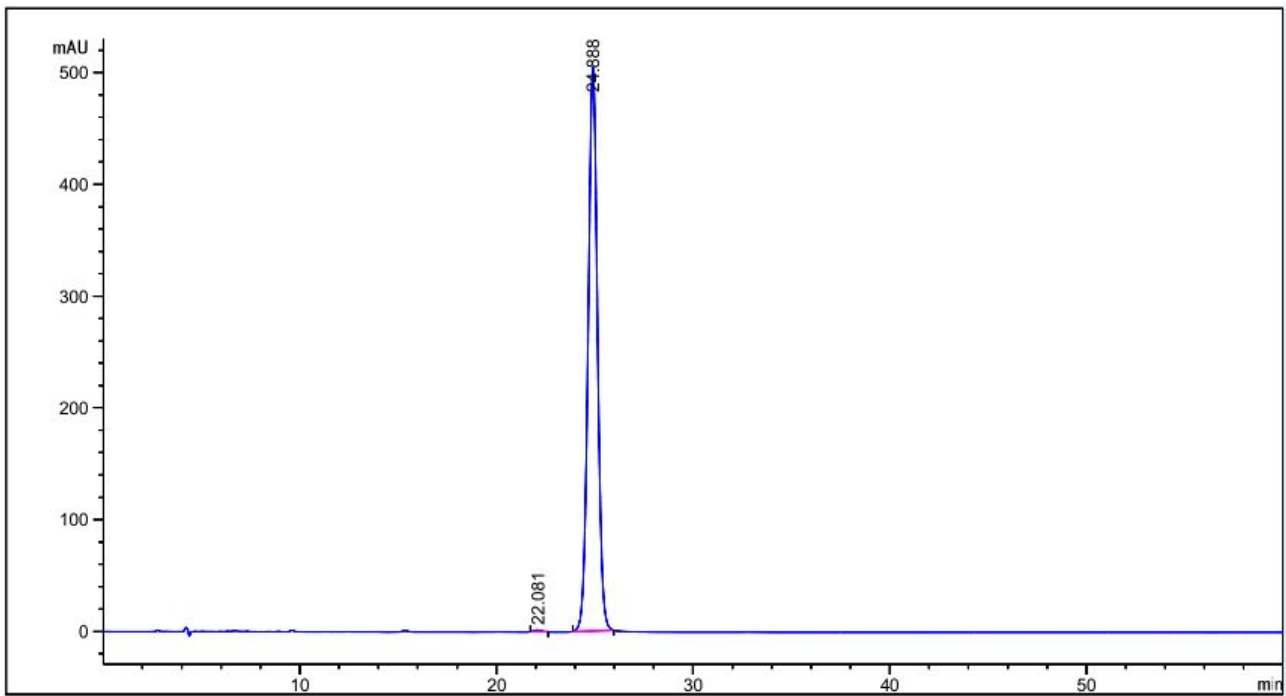
排序 : 信号
乘积因子 : 1.0000
稀释因子 : 1.0000
内标使用乘积因子和稀释因子

信号 1: DAD1 B, Sig=245,8 Ref=600,100

峰 #	保留时间 [min]	类型	峰宽 [min]	峰面积 [mAU*s]	峰高 [mAU]	峰面积 %
1	8.405	BB	0.1939	1.01075e4	797.35522	99.6091
2	10.076	BB	0.2270	39.66961	2.70633	0.3909

总量 : 1.01472e4 800.06155

HPLC of the compound 13



面积百分比报告

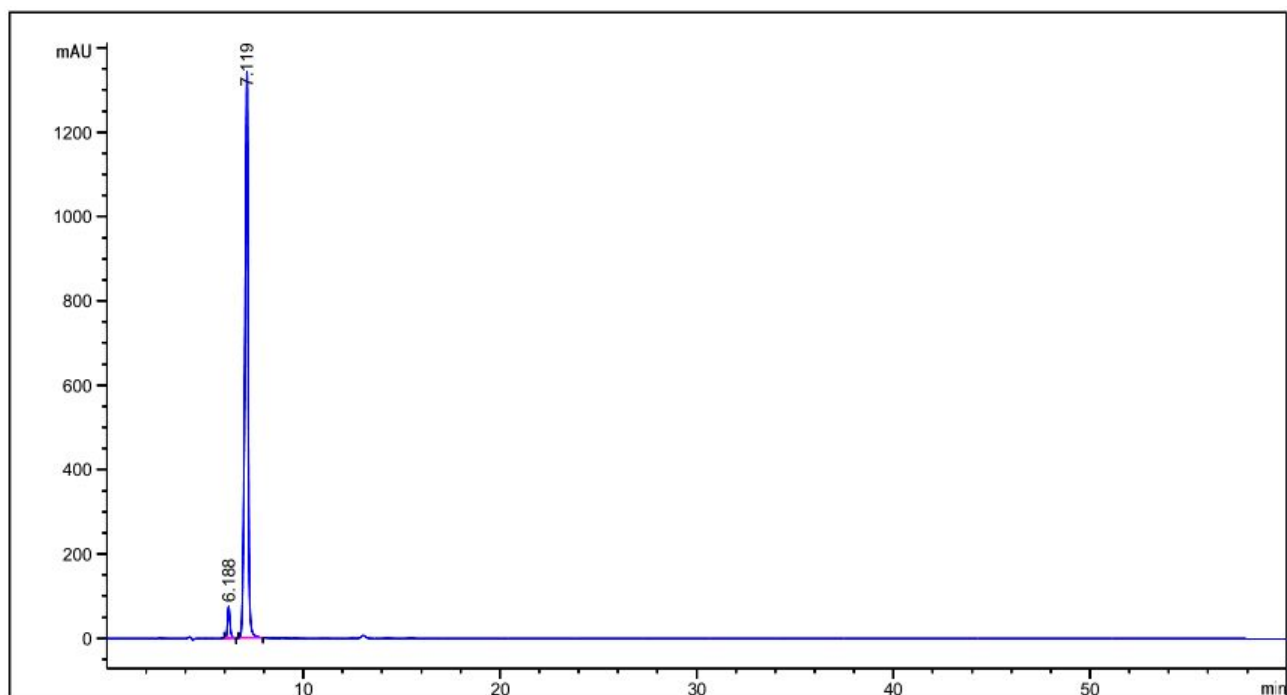
排序 : 信号
乘积因子 : 1.0000
稀释因子 : 1.0000
内标使用乘积因子和稀释因子

信号 1: DAD1 B, Sig=245,8 Ref=600,100

峰 #	保留时间 [min]	类型	峰宽 [min]	峰面积 [mAU*s]	峰高 [mAU]	峰面积 %
1	22.081	BB	0.3767	41.58191	1.61355	0.2476
2	24.888	BB	0.5072	1.67497e4	504.63580	99.7524

总量 : 1.67913e4 506.24935

HPLC of the compound 15



面积百分比报告

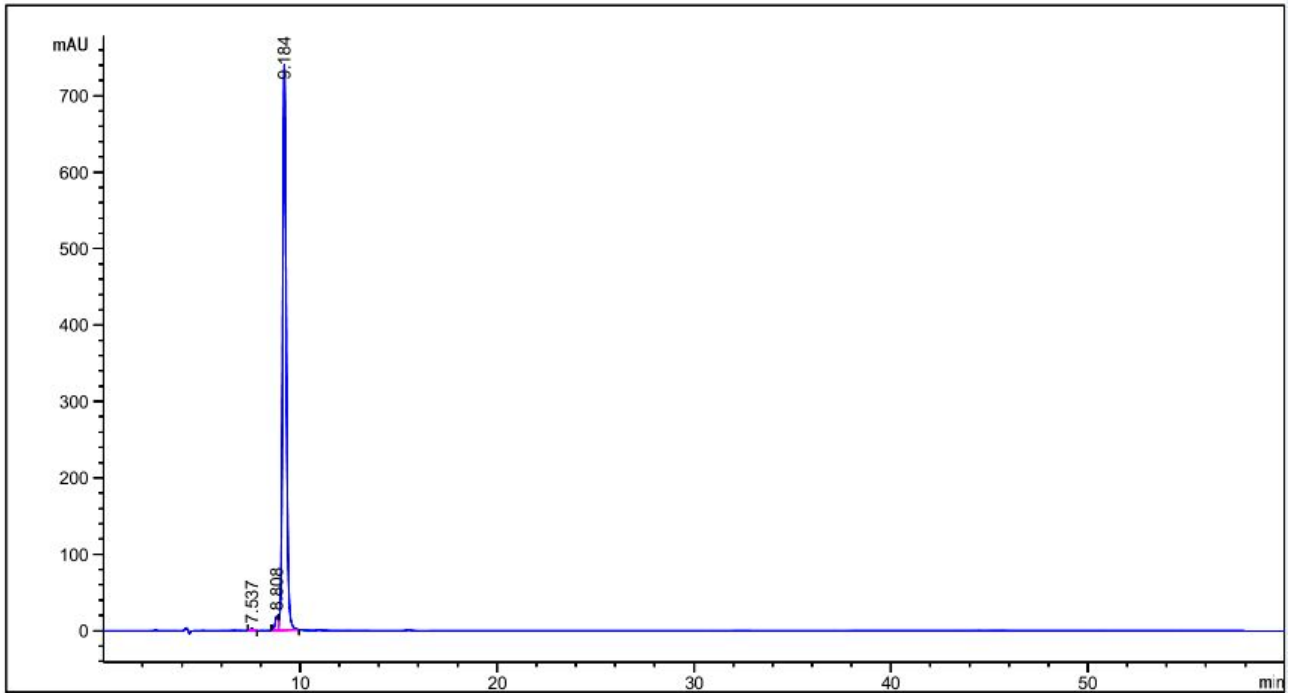
排序 : 信号
乘积因子 : 1.0000
稀释因子 : 1.0000
内标使用乘积因子和稀释因子

信号 1: DAD1 B, Sig=245,8 Ref=600,100

峰 #	保留时间 [min]	类型	峰宽 [min]	峰面积 [mAU*s]	峰高 [mAU]	峰面积 %
1	6.188	VB	0.1329	661.24878	74.94682	4.1464
2	7.119	BB	0.1687	1.52865e4	1344.33643	95.8536

总量 : 1.59477e4 1419.28324

HPLC of the compound 18



面积百分比报告

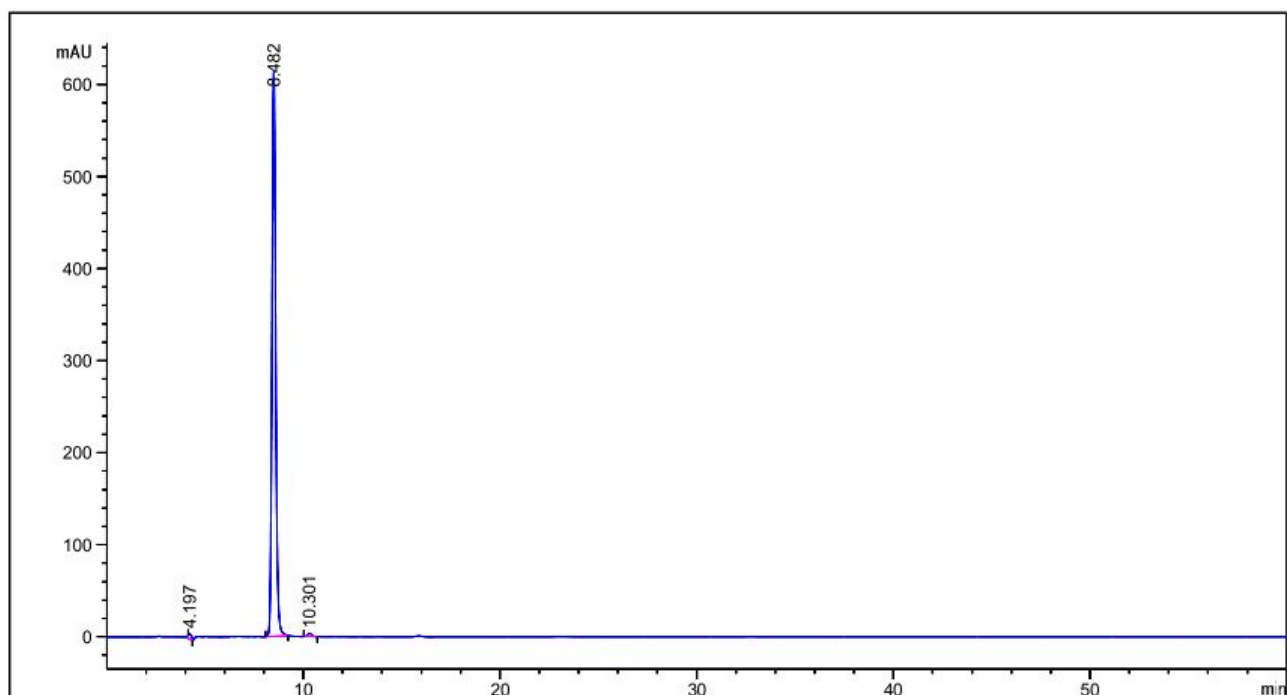
排序 : 信号
乘积因子 : 1.0000
稀释因子 : 1.0000
内标使用乘积因子和稀释因子

信号 1: DAD1 B, Sig=245,8 Ref=600,100

峰 #	保留时间 [min]	类型	峰宽 [min]	峰面积 [mAU*s]	峰高 [mAU]	峰面积 %
1	7.537	BB	0.1624	32.99413	3.09491	0.3356
2	8.808	BV	0.1718	212.81509	19.13340	2.1649
3	9.184	VB	0.1970	9584.59668	740.72864	97.4995

总量 : 9830.40590 762.95695

HPLC of the compound 24



面积百分比报告

排序 : 信号
 乘积因子 : 1.0000
 稀释因子 : 1.0000
 内标使用乘积因子和稀释因子

信号 1: DAD1 B, Sig=245,8 Ref=600,100

峰 #	保留时间 [min]	类型	峰宽 [min]	峰面积 [mAU*s]	峰高 [mAU]	峰面积 %
1	4.197	VV	0.1208	57.20350	6.25036	0.7069
2	8.482	BB	0.1998	7980.43408	613.22455	98.6188
3	10.301	BB	0.2342	54.56830	3.61273	0.6743

总量 : 8092.20588 623.08763

Molecular modeling

Most of the PDE4 inhibitors described to date, including Rolipram and the FDA-approved roflumilast, inhibit all four subfamilies of PDE4. To further understand the binding mode of these Rolipram-Tanilast hybrids, the most active compound **5**, was selected and docked into the PDE4D catalytic pocket (PDB code: 1xoq)¹ using the molecular docking approach glide SP mode.^{2, 3}

As shown in Figure 1, the scaffold 4-(cyclopentyloxy)-3-methoxyphenyl group of compound **5** and Rolipram shared similar binding conformations (Figure 1A), these interactions were similar to those of Rolipram (Figure 1B) and were considered as the essential interactions for PDE4 inhibitors.⁴ While, comparing to Rolipram, compound **5** formed additional two hydrogen bonds with Asp 318 and Tyr 159 (Figure 1A, B), which might explain its higher potency than that of Rolipram. This model was generally congruent with the above-summarized SARs. The formation of 2H-pyran ring D enhanced the H-bond interactions with the protein residues (Tyr 159 and Asp 318) and thus generated good activity, while the lack of free phenolic hydroxyls at C-5 or C-4' would disturb their hydrogen bond interactions with Gln 369, His 160 or Asp 318, which accounted for a dramatic decrease of the activity.

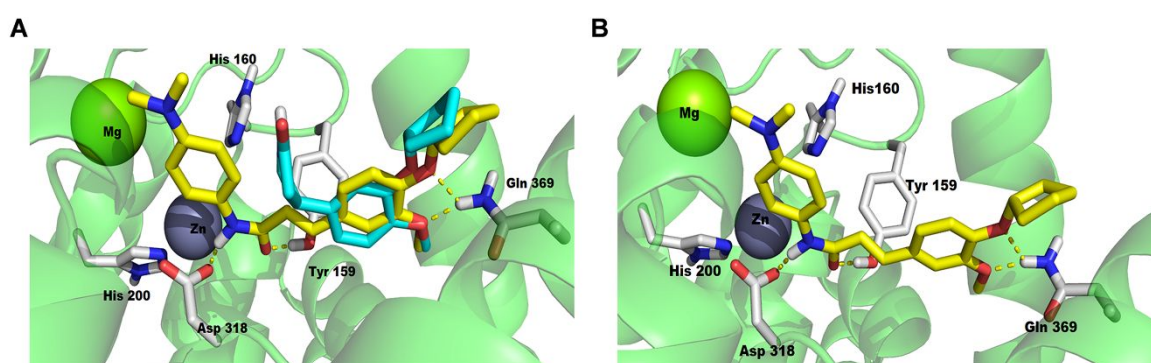


Figure S1. Binding modes of ligands with PDE4D catalytic pocket (PDB code: 1xoq) derived from docking simulations (yellow dashed lines for hydrogen bond). Interactions are displayed by yellow dotted lines. Key residues that could form interactions with compound **5** are shown. (A) Comparing binding mode of compound **5** (yellow) and Rolipram (cyan). (B) Binding mode of compound **5**.

Kinase activity assay

These assays were carried out as described previously.⁵ All of the enzymatic reactions were conducted at 25°C for 60 mins. The 50 μ L reaction mixture contains 40 mM MOPS, pH 7.5, 0.5 mM EDTA, 15 mM MgCl₂, 0.15 mg/mL BSA, 1 mM DTT, 0.05% Proclin 200, 15 ng/mL PDE4 CAT and 100 nM FAM-Cyclic-3', 5' -AMP. The compounds were diluted in 10% DMSO and 5 μ L of the dilution was added to a 50 μ L reaction so that the final concentration of DMSO is 1% in all of reactions. The reaction mixture was incubated at 25°C for 1 h. Then add 100 L diluted binding agent to each well and incubate at 25°C for 1 h with slow shaking. Read the fluorescence polarization of the sample used an excitation filter of 360 nm and an emission filter of 480 nm. The IC₅₀ values were calculated using nonlinear regression with normalized dose–response fit using Prism GraphPad software.

Table S1. PDE4B2 and PDE4D7 kinase activity assay of compound 5.

Kinase target	PDE4B2	PDE4D7
Inhibition (%)	0	6

References

- (1). Card, G. L., England, B. P., Suzuki, Y., Fong, D., Powell, B., Lee, B., Luu, C., Tabrizizad, M., Gillette, S., Ibrahim, P. N., Artis, D. R., Bollag, G., Milburn, M. V., Kim, S. H., Schlessinger, J., Zhang, K. Y. J., (2004) Structural basis for the activity of drugs that inhibit phosphodiesterases. *Structure* 12, 2233-2247.
- (2). Friesner, R. A., Banks, J. L., Murphy, R. B., Halgren, T. A., Klicic, J. J., Mainz, D. T., Repasky, M. P., Knoll, E. H., Shelley, M., Perry, J. K., Shaw, D. E., Francis, P., Shenkin, P. S., (2004) Glide: a new approach for rapid, accurate docking and scoring. 1. Method and assessment of docking accuracy. *J. Med. Chem.* 47, 1739-1749.
- (3). Halgren, T. A., Murphy, R. B., Friesner, R. A., Beard, H. S., Frye, L. L., Pollard, W. T., Banks, J. L., (2004) Glide: a new approach for rapid, accurate docking and scoring. 2. Enrichment factors in database screening. *J. Med. Chem.* 47, 1750-1759.
- (4). Huai, Q., Wang, H. C.; Sun, Y. J., Kim, H. Y., Liu, Y. D., Ke, H. M., (2003) Three-dimensional structures of PDE4D in complex with roliprams and implication on inhibitor selectivity. *Structure* 11, 865-873.
- (5). Huang, W., Zhang, Y., Sportsman, JR., (2002) A fluorescence polarization assay for cyclic nucleotide phosphodiesterases. *J. Biomol. Screen.* 7, 3, 215–222.